HIGH ENERGY PHYSICS DIVISION SEMIANNUAL REPORT OF RESEARCH ACTIVITIES

July 1, 2002 – December 31, 2002

Argonne National Laboratory, with facilities in the states of Illinois and Idaho, is owned by the United States government, and operated by The University of Chicago under the provisions of a contract with the Department of Energy.

Available electronically at http://www.doe.gov/bridge

Available for a processing fee to U.S. Department of Energy and its contractors, in paper, from:

U.S. Department of Energy
Office of Scientific and Technical Information
P.O. Box 62
Oak Ridge, TN 37831-0062
phone: (865) 576-8401
fax: (865) 576-5728
email: reports@adonis.osti.gov

Argonne National Laboratory
9700 South Cass Avenue
Argonne, Illinois 60439

HIGH ENERGY PHYSICS DIVISION
SEMIANNUAL REPORT OF
RESEARCH ACTIVITIES

July 1, 2002 - December 31, 2002

Prepared from information gathered and edited by
The Committee for Publications and Information:

Members: P. Malhotra
             J. Norem
             R. Rezmer
             R. Wagner

July 2003

Abstract

This report describes the research conducted in the High Energy Physics Division of Argonne National Laboratory during the period of July 1 through December 31, 2002. Topics covered here include experimental and theoretical particle physics, advanced accelerator physics, detector development, and experimental facilities research. Lists of Division publications and colloquia are included.

Table of Contents

I. EXPERIMENTAL RESEARCH PROGRAM

I.A. EXPERIMENTS WITH DATA

I.A.1. Medium Energy Polarization Program

During the period July - December, 2002, there were preparations at RHIC and STAR for the upcoming d + Au run, which began early in 2003. A number of papers were published with authors from the spin group, and analysis of polarimeter data from the past polarized proton run occurred. The continuing work on construction and testing of shower maximum detector modules for the STAR endcap electromagnetic calorimeter is described in another section of this report.

A paper on Brookhaven experiment E950 was published (Phys. Rev. Lett. **89**, 052302 (2002)) with an Argonne author. This experiment calibrated a CNI polarimeter in the AGS at the extraction energy using a very thin carbon ribbon target. Results from an ANL-led experiment in an external beam (E925), that ran at about the same time, were crucial for this calibration. The data shown in Fig. 1 indicate a sizeable hadronic spin-flip contribution exists for very small angle p + carbon elastic scattering, which is surprising. These results are being used to transfer the polarimeter calibration to RHIC at the injection momentum of $p_{lab} = 24$ GeV/c.
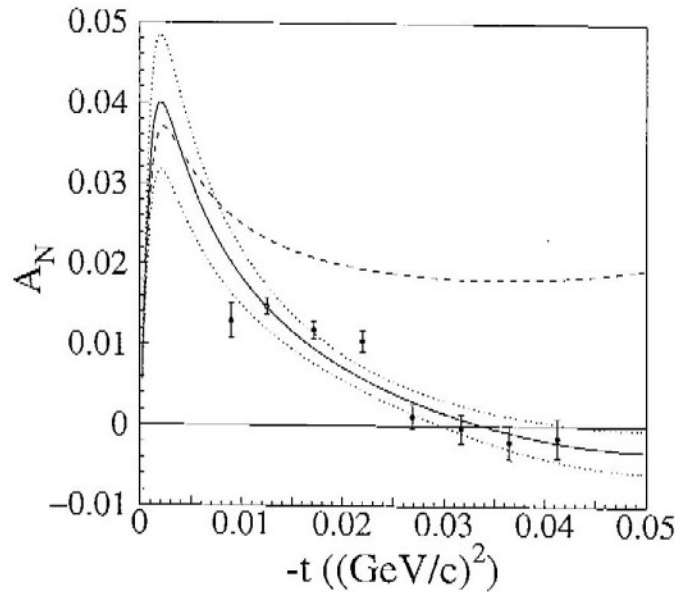
Figure 1. The analyzing power in p + C elastic scattering as a function of 4-momentum transfer squared, t, at 22 GeV/c beam momentum. The error bars on the data points are statistical only. The dashed line is the theoretical function with no hadronic spin-flip amplitude. The solid line is the fitted function from theory, and the dotted lines are the one-sigma error band of the fitted result.

Several papers on STAR results were published and several others submitted for publication. Two discuss strange particle production in heavy ion collisions ("Midrapidity Λ and $\overline{\Lambda}$ Production in Au + Au Collisions at $\sqrt{s_{NN}}$ = 130 GeV," Phys. Rev. Lett. **89**, 092301 (2002) and "K^{*0} (892) Production in Relativistic Heavy ion Collisions at $\sqrt{s_{NN}}$ = 130 GeV," Phys. Rev. **C66**, 061901 (R) (2002)). This is the first observation of K^{*0}(892) in heavy ion collisions, and the production cross section is comparable to theoretical expectations without rescattering of decay daughters in a dense medium. The $\overline{\Lambda}$ yield increases relative to negatively charged hadrons as a function of p_T, which cannot be described by existing perturbative QCD inspired string fragmentation models alone.

Two other papers describe properties of elliptic flow in heavy ion reactions ("Elliptic Flow from Two- and Four-Particle Correlations in Au + Au Collisions at $\sqrt{s_{NN}}$ = 130 GeV," Phys. Rev. **C66**, 034904 (2002) and "Azimuthal Anisotropy of K_s^0 and $\Lambda + \overline{\Lambda}$ Production at Midrapidity from Au + Au Collisions at $\sqrt{s_{NN}}$ = 130 GeV," Phys. Rev. Lett. **89**, 132301 (2002)). The first presents an estimate of the non-flow correlations in the azimuthal anisotropy parameter, v_2, in the momentum distribution; such correlations are about 15% and are present throughout the measured range of p_T and η. The second paper shows that v_2 for the three strange particle types discussed are adequately described by hydrodynamic models for $p_T \leq 2$ GeV/c, but they saturate above this momentum; see Fig. 2.
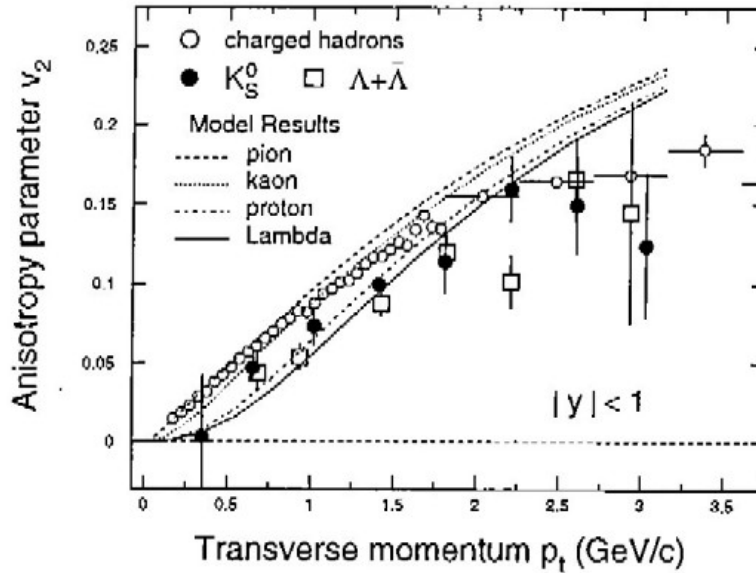
Figure 2. Elliptic flow v_2 as a function of p_T for the strange particles K_s^0 (filled circles) and $\Lambda + \overline{\Lambda}$ (open squares) from minimum bias Au + Au collisions. For comparison, the open circles are for all charged hadrons. The lines are from hydrodynamic model calculations. Error bars shown are statistical uncertainties only.

The first measurements of coherent ρ° production with and without accompanying nuclear excitation, Au Au $\rightarrow$ Au* Au* ρ° and Au Au $\rightarrow$ Au Au ρ°, are reported in the paper "Coherent ρ° Production in Ultraperipheral Heavy-Ion Collisions" (Phys. Rev. Lett. **89**, 272302 (2002)). The data confirm the existence of vector meson production in ultraperipheral heavy-ion collisions. The ρ° are produced at small p_T, showing the coherent coupling to both nuclei. The cross sections at $\sqrt{s_{NN}}$ = 130 GeV are in agreement with theoretical calculations, and the total is $0.46 \pm 0.22 \pm 0.11$ barns!

The sixth STAR paper was "Centrality Dependence of High-p_T Hadron Suppression in Au + Au Collisions at $\sqrt{s_{NN}}$ = 130 GeV" (Phys. Rev. Lett. **89**, 202301 (2002)). The inclusive charged hadron yield was measured for $|\eta| < 0.5$ as a function of transverse momentum and centrality (based on primary charged particle multiplicity, where the most central bin of 0-5% corresponds to the highest multiplicity). Figure 3 shows the ratio of the Au + Au yield to the pp yield, corrected for collision geometry via the factor $T_{AA} = <N_{binary}>/ \sigma_{inel}^{NN}$, which is the ratio of the equivalent number of binary nucleon-nucleon collisions to the inelastic NN cross section. At high p_T, hadron yields scale with $<N_{binary}>$ for peripheral collisions, but there is increasing suppression for more central events. This may indicate substantial energy loss of final state partons or hadrons in the medium generated by relativistic heavy ion collisions.

Data analysis continued at Argonne and Valparaiso University on the reaction K$^-$ p $\rightarrow$ π° Σ° at eight momenta between 500 – 750 MeV/c from the Crystal Ball. Both differential cross sections and Σ° polarizations are being derived. The data sample is approximately an order of magnitude larger than obtained previously with bubble chambers. Analysis of data from the AGS and the RHIC CNI polarimeters also continued, and reports are being prepared to summarize the results.
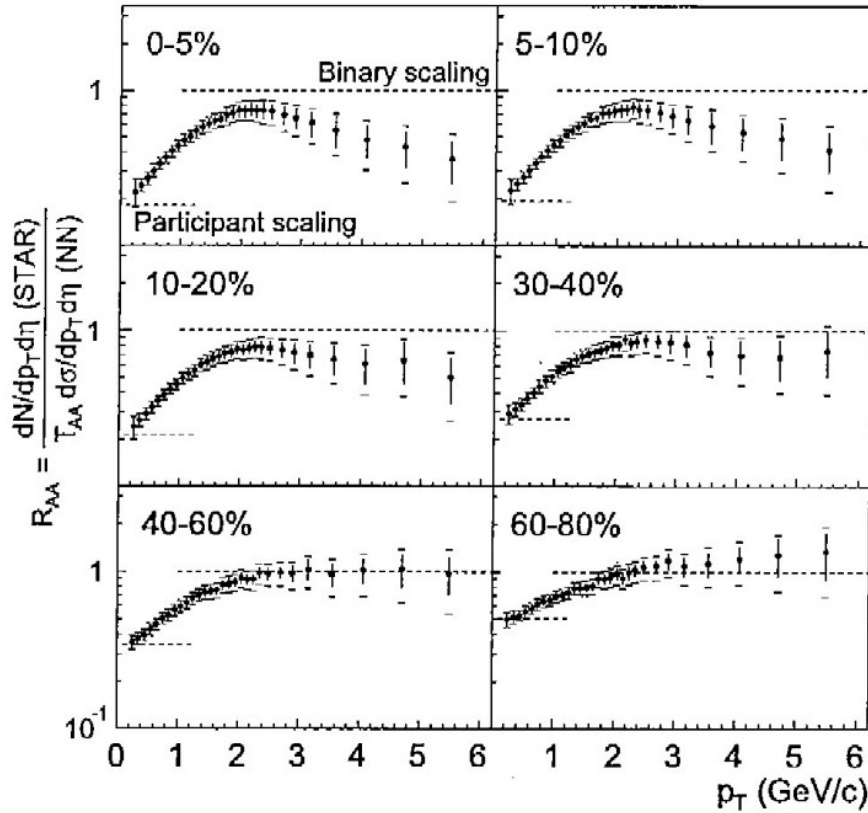
Figures 3. Ratio of charged particle yields for Au + Au relative to NN collisions, corrected for collision geometry, in various centrality classes. The error bars are the systematic uncertainties of the measured spectra, while the caps show their quadrature sum with the systematic uncertainty of the NN reference data. Errors between different centrality and transverse momentum bins are highly correlated.

(H. Spinka)

I.A.2   Collider Detector at Fermilab

a)   Physics

The quality of the new data continues to be good enough for physics. Samples of about 72 pb^{-1} were created for analyses aimed at the winter conferences. As the sample size is still disappointing, many of the analyses were literally exercises for the students, but a few had some physics interest beyond demonstrating at some low level that the program is alive again. Samples have finally gotten big enough to provoke the embarrassing question, "have you combined that result with Run 1?"

The W and Z boson cross sections are both of physics interest; they should be higher with the increased energy, and they may provide a better luminosity normalization than the inelastic cross section. They also provide the basic understanding of electrons, muons, tau's, and missing transverse energy which are needed for top studies and new physics searches. The cross section times leptonic branching ratio for Ws at 1.96 TeV is predicted at NNLO to be 2.69 ±0.10 nb, while the winter conference measurements are 2.64 ±0.01 (stat) ±0.09 (sys) for electrons, 2.64. ±0.02 (stat) ±0.12 (sys) for muons, and 2.62 ±0.07 (stat) ±0.21 (sys) for tau's. Note that an additional 6% luminosity normalization uncertainty applies to all cross section measurements. The corresponding prediction for Z's is 252 ±9 pb. The electron peak is shown in Fig. 1 and illustrates good calorimeter resolution; the
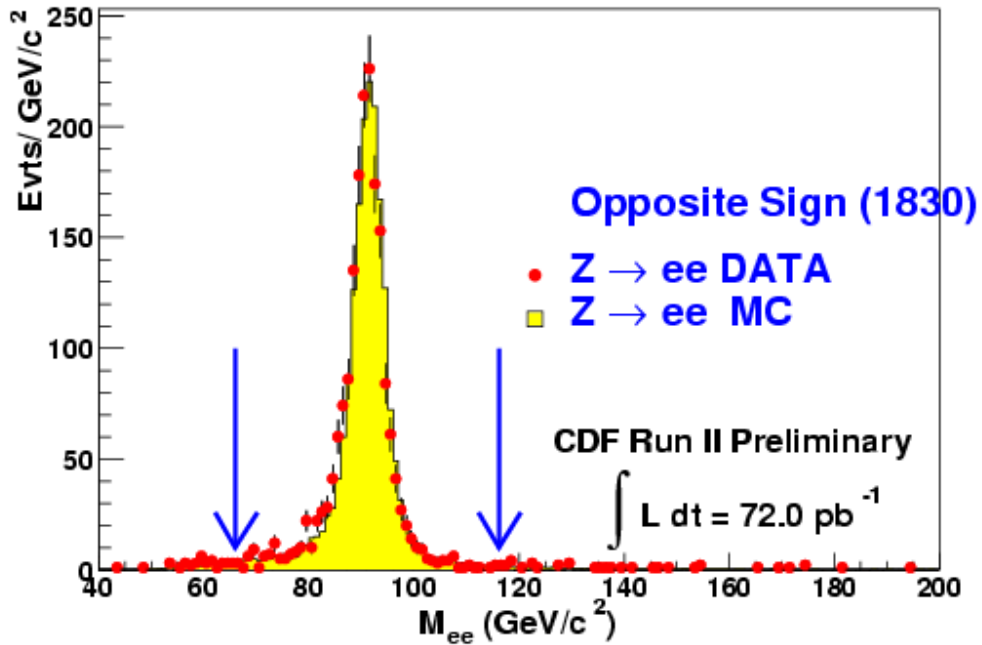
Figure 1. Dielectron mass distribution used for the Z cross section.

measured cross section times B.R. is 267 ±6 (stat) ±15 (sys). The electron studies provide alignment corrections for tracking, which are important for resolution at high momentum, as illustrated by the muon Z peak shown in Fig. 2; this peak corresponds to a cross section times B.R. of 246 ±6 (stat) ±12 (sys).
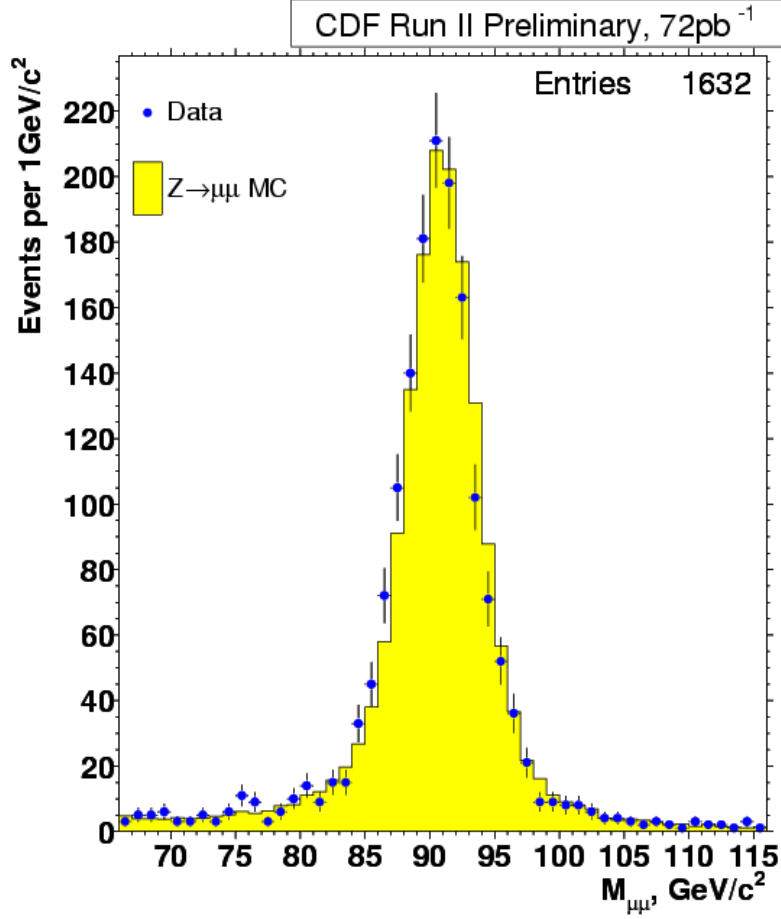
Figure 2. Dimuon invariant mass used for the Z cross section.

The integration of the silicon detector in the data taking has improved continuously. The fraction of the detector that is actually working, and the ability of the silicon impact parameter trigger (SVT) to take advantage of this coverage, have all been improving. The all-hadronic heavy flavor program based on the SVT is new for Run II; it represents a unique development in hadron collider physics. The flagship effort toward Bs mixing will need increased detector efficiency, improved trigger strategy, and much more recorded luminosity. The rapid oscillation will also require the vertex accuracy from the innermost silicon, not yet functional offline. However, the signal is there, shown in Fig. 3, so the flagship program is started, along with a large variety of hadronic charm and bottom studies.
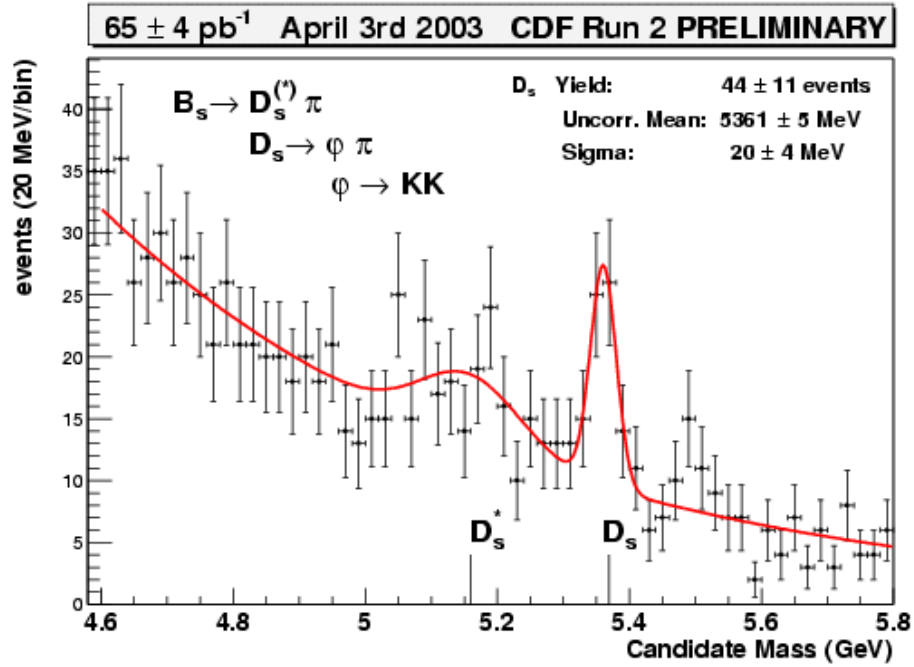
Figure 3. Bs candidate peak in the mode shown. So far we are getting less than an event per inverse picobarn.

Studies of heavy flavor production at the Tevatron have already produced unexpected results. For example, the B-production cross sections, measured with exclusive J/ψ decay modes, turn out to be larger than next-to-leading order calculations by a factor of three. This is observed for high p_T B-production, but it is not known whether this applies to the total B cross section integrated over all values of p_T. Likewise, the cross sections for direct onium production (J/ψ and ψ (2S)) are about 100 times larger than the original predictions of color-singlet models; this observation helped spur the development of color-octet expansions in non-relativistic QCD theory (NRQCD). The NRQCD theory predicts both the p_T dependence and the spin alignment for different contributions in the expansion.

In the Run II CDF trigger, we have arranged to lower the p_T threshold for muons from 2 GeV/c (Run I value) down to 1.5 GeV/c, i.e. less than half the J/ψ mass. This in turn allows CDF to trigger on J/ψ's down to p_T=0 in the center of mass. Fig. 4 shows the dimuon mass spectrum for events in the lowest p_T J/ψ bin (0<p_T<250 MeV/c) A clean J/ψ signal is evident.
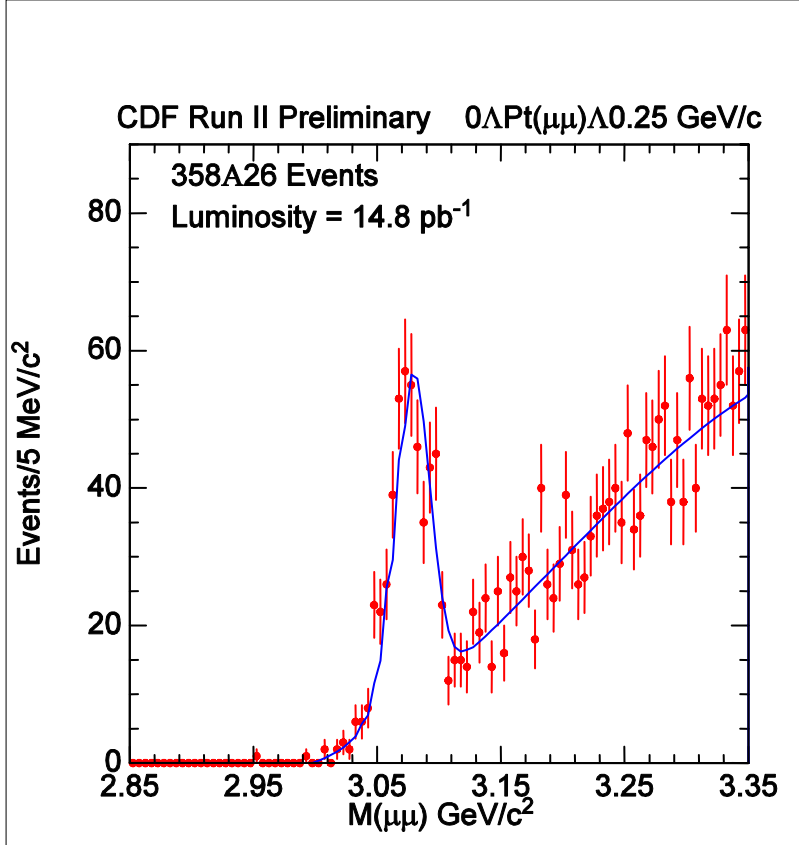
Figure 4. Invariant mass of dimuon pairs of total transverse momentum between zero and 250 MeV/c^2 showing a J/ψ yield of 358 ±26 events.

Fig. 5 shows the p_T distribution for the J/ψ signal. Most of the spectrum is below 5 GeV/c, which was the lowest p_T value used in the run I analyses. We have used these data to measure the differential cross section over the entire p_T range, and we have used the J/ψ lifetime to separate indirect production from B-hadron decays from the direct onium production. We plan to use a deconvolution of the long-lived spectrum to measure the B-production cross section down to p_T=0, and thereby establish the total B-production cross section.

The most powerful new feature of the CDF detector has been the ability to trigger directly on tracks having detached vertices as measured in the silicon vertex detector. These triggers are highly enriched in heavy flavor bottom and charm decays. One example is the "lepton+SVT" trigger; this trigger requires a lepton (electron or muon) with p_T> 4 GeV/c, accompanied by at least one detached track with p_T>2 GeV/c. This trigger is designed to collect
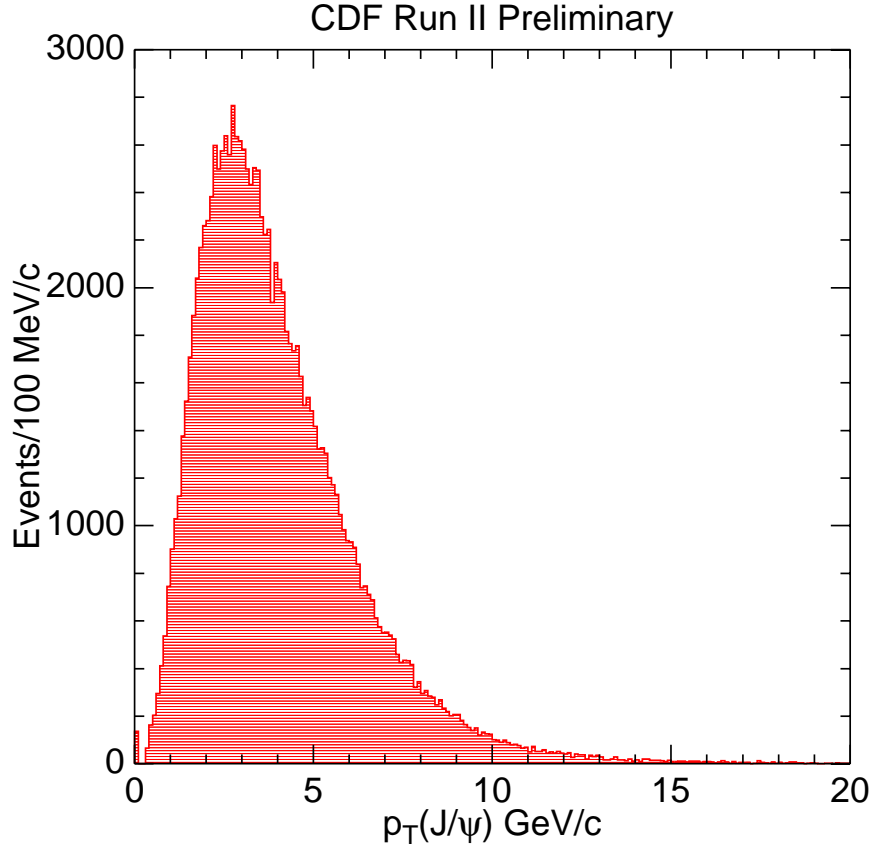
Figure 5. Transverse momentum of the J/ψ events.

a large sample of inclusive semileptonic B-hadron decays, where the lepton comes from the primary B decay, and the detached track comes from a secondary charm vertex; there is no trigger bias on the impact parameter of the lepton itself. In addition, this trigger also collects semileptonic decays of directly produced charm, as well as fake leptons accompanied by mismeasured tracks or tracks from K_S or Λ decays. It is straightforward to search for exclusive semileptonic B decays by identifying charm hadrons (D^0, D^+, D_S, and Λ_C); the measured yields for these decays exceed those in run I by about a factor of five. The total inclusive sample is also very useful for studies of flavor tagging. By separating out the B-hadron decay contribution to the sample, we can obtain a very high statistics inclusive B sample; we search the away side hemisphere in these events for flavor tag signatures, including electrons, muons, and kaons via time-of-flight. Fig. 6 shows the mass spectrum of the lepton with the accompanying displaced
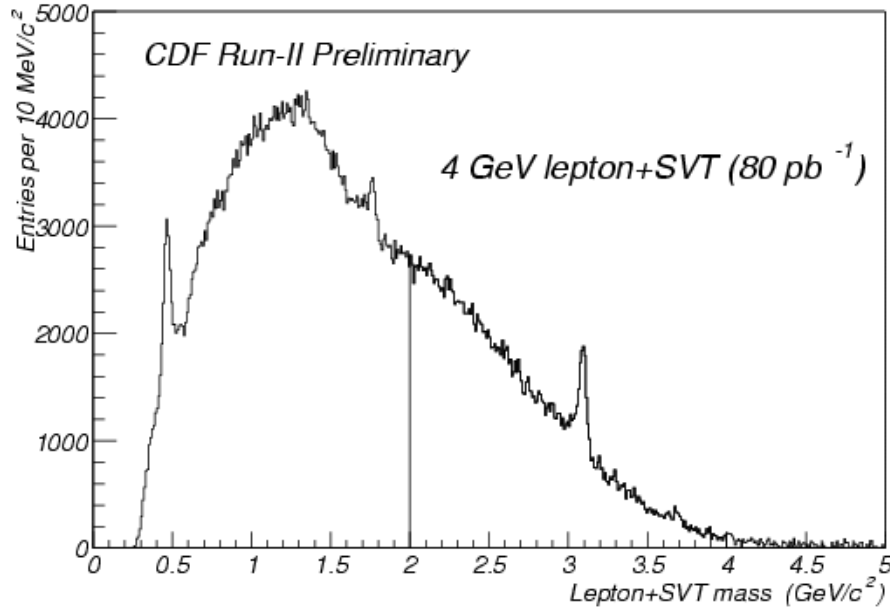
Figure 6. Mass of the lepton and displaced track for 4 GeV lepton plus SVT track triggers.

track. We use a subtraction technique to remove fake lepton events and also charm-anticharm events in which the lepton and the track come from different parents. With a mass cut M(lepton-track)>2 GeV, indicated by the shaded region, we can isolate a pure B decay component. The region below 2 GeV is a mixture of B decays and direct charm, as evidenced by the lifetime distributions. In addition, the spectrum shows three peaks: the J/ψ peak, in which the detached track is itself a lepton, and where the J/ψ comes from B decay; a K_S peak, in which the lepton candidate is actually a pion fake; and a D$^\circ$ peak, in which the lepton is actually a pion or kaon fake. Both the D$^\circ$ and the K_S signals are copious and have a high probability of passing the SVT trigger, and they provide an expedient way to measure directly the fake lepton backgrounds in the sample.
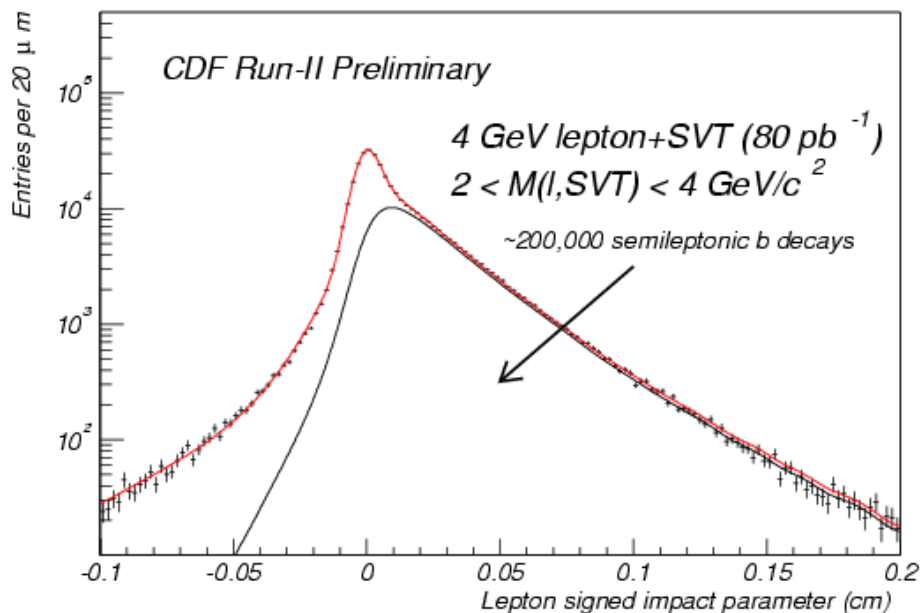
Figure 7. Signed impact parameter distribution for displaced tracks from 2 to 4 GeV lepton plus displaced track events. The b lifetime contribution indicates the b yield.

Fig. 7 shows the lepton impact parameter distribution for the high mass sample, together with a fit that includes B decays, direct charm, fake leptons, and charm-anticharm contributions. The peak at zero impact parameter is due to fake leptons. The negative impact parameter tail is due mainly to the charm-anticharm component. With the mass cut, the fits are consistent with no direct charm component. Finally, the shaded region in Fig. 7 shows the B hadron contribution returned by the fits. The fits agree well with the data, and give a total signal of 200,000 (2.5 nb.) B decay events. The non-B components can be removed by the subtraction technique used for Fig. 6. The sample is now being used to validate the various flavor tagging techniques.

Larry Nodulman is using the understanding of calorimeter data to help understand the top mass and W mass measurements. Barry Wicklund, Masa Tanaka, Tom LeCompte, Bob Wagner, and Karen Byrum are working on various aspects of b physics, and Bob Blair and Steve Kuhlmann continue their interest in photon physics. Steve continues to lead the dijet mass optimization effort, but the prospects for Higgs detection seem to be receding.

b) The CDF Operations

Steady if slow data taking of physics quality continued. Jimmy Proudfoot's operational concerns as Deputy Head of CDF Operations included monitoring data quality, increasing operational efficiency, and developing the trigger and DAQ bandwidth. There has been considerable progress in all those areas. Increasing luminosity remained mostly an academic issue. Larry Nodulman served as co leader ("SPL") for calorimeter operations.

Karen Byrum, with help from Steve Kuhlmann, Jimmy Proudfoot and Larry Nodulman and Gary Drake and company, continued to lead the ongoing support for shower max readout operations; this continued to be a reasonably stable operational equilibrium.

Our electronics in the Level 2 trigger, the shower max trigger and the isolation trigger, continued operations supported by Masa Tanaka, Karen Byrum, Steve Kuhlmann and Bob Blair. Masa has agreed to take on the role of operations manager for CDF for the spring.

Larry Nodulman worked with members of the Electron Task Force to monitor the performance of the central EM calorimeter. The overall energy scale fell slowly during the period, and the online scale factor was increased by 3% to keep the trigger gain close to being correct. The gains for individual towers were rather uniform after pmt gains were downloaded. Detailed run dependence from inclusive electrons are provided for use offline.

Bob Wagner continued to head the offline electron and photon software effort. He also, along with Barry Wicklund and Larry Nodulman, worked with the Electron Task Force to define electrons correctly and provide convenient access to the relevant numbers derived from the data. Most of the emphasis of the Electron Task Force has been on utilizing the plug region.

Barry Wicklund was also a leader of the B physics trigger strategy group. Improvements of the capabilities and strategy for triggering on tracks with impact parameter are continuing.

(L. Nodulman)

I.A.3. The CDF Upgrade Project

a) Run IIb Planning

The overall efforts for Run 2b had a baseline Lehmann review in October. Steve Kuhmann is the Level 2 manager for calorimeters, which also includes the EM timing upgrade, as well as taking a leading role in the preradiator project. The preradiator upgrade, with considerable support from Japan, Italy and Russia, passed baseline and prototypes were designed and begun. The MINOS test stand at Argonne will be modified to do development and production quality control. Design work and planning for production at Argonne are well under way.

Jimmy Proudfoot and Bob Blair developed a plan to use ATLAS ROI builder technology as part of the DAQ upgrade; this fits in well with the new Level 2 trigger scheme. We looked at the possibility of involvement on silicon electronics but a good match to our shop's capabilities was not found.

(L. Nodulman)

I.A.4. Non-Accelerator Physics at Soudan

In July 2001, the Soudan-2 experiment completed the taking of data using its fine-grained iron tracking calorimeter of total mass 963 tons. Analysis is continuing on the atmospheric flavor ratio and its implications for oscillations, as well as proton decay. The total data exposure was 5.9 fiducial kiloton-years (kTy). Results presented here are based upon the full 5.9 kTy exposure. We have recently finished our analysis of horizontal muons, which has implications for the atmospheric neutrino flux, as well as the possibility that very high energy neutrinos are coming from distant cosmological sources such as Active Galactic Nuclei (AGNs).

There were approximately 10^8 triggered events in the Soudan 2 detector in the data set considered for this analysis. About half of these were due to cosmic ray muons, and half due to radioactivity in different parts of the detector which satisfied the trigger due to multiplexing. These events were processed using a pattern recognition filter code which identifies muon tracks and discriminates against unphysical background from noise. Five additional cuts were then applied to define a "horizontal muon" sample. Tracks were required to have end points consistent with a particle entering and leaving the detector. Acceptable track ends were required to (1) lie outside the fiducial volume which is 50 cm from the edge of the main detector, or (2) lie on a module boundary inside of the main detector and (3) point to a coincident shield hit or (4) point to a portion of the shield where a shield module did not exist. The azimuth cut rejected noise events which reconstructed parallel to the axes of the detector. A zenith cut defined the sample of horizontal muons. A track length cut minimized short tracks such as pions that originated from nuclear interactions within the rock nearby and also low energy cosmic ray muons which had undergone large multiple Coulomb scattering. The anode-width cut rejected events that were primarily along one anode wire. These were actually along the north-south direction in azimuth, but they were often mis-reconstructed. The efficiency of these cuts for Monte Carlo muons generated isotropically with zenith angles θ_z exceeding $82°$is 0.56 ± 0.01.

The pattern recognition software found single horizontal muon tracks, but it also kept a variety of background events. Most background events contained short horizontal tracks accompanied by other activity in the detector. Physicist scanning of all tracks greater than $78°$ was done to verify the track fits and to eliminate obvious backgrounds. Common backgrounds were due to certain patterns of electronic noise, vertical muons undergoing large radiative stochastic losses, multiple muons, and neutrino interactions within the detector. Tracks with visible multiple scattering (greater than $2°$) or with in-time shield hits that were not due to a horizontal muon were also rejected. All events were subjected to two independent scans and residual discrepancies were rescanned. The scan rejected 58% of data events output from the filter. The uncorrelated scan inefficiency as determined from the double scan was less than 1%. The scan efficiency was calculated to be 95%. The dominant loss was due to multiple scattering by more than $2°$ within the Soudan 2 detector by those muons with the lowest energies.

The track-length cut of 1.75 m (2.2 hadronic interaction lengths) minimized the number of short tracks which arose from processes which were not neutrino-related. The latter backgrounds included pion tracks originating from deep inelastic muon scattering within nearby rock, or else high energy cosmic ray muons from vertical directions which experienced large-angle multiple scattering. This length corresponds to a muon energy threshold of 400 MeV, but the restriction on multiple scattering raised this to an effective threshold of 1.8 GeV.

The number of accepted events after scanning, with $\theta_z > 78°$, was 1237 events. The slant depth cut of 14 kmwe reduced this sample to 65 events. The track length, azimuth and zenith angle distributions of all 1237 events are shown in Figure 1. The depletions at regular intervals on azimuthal projections of these plots are due to the azimuth cuts.
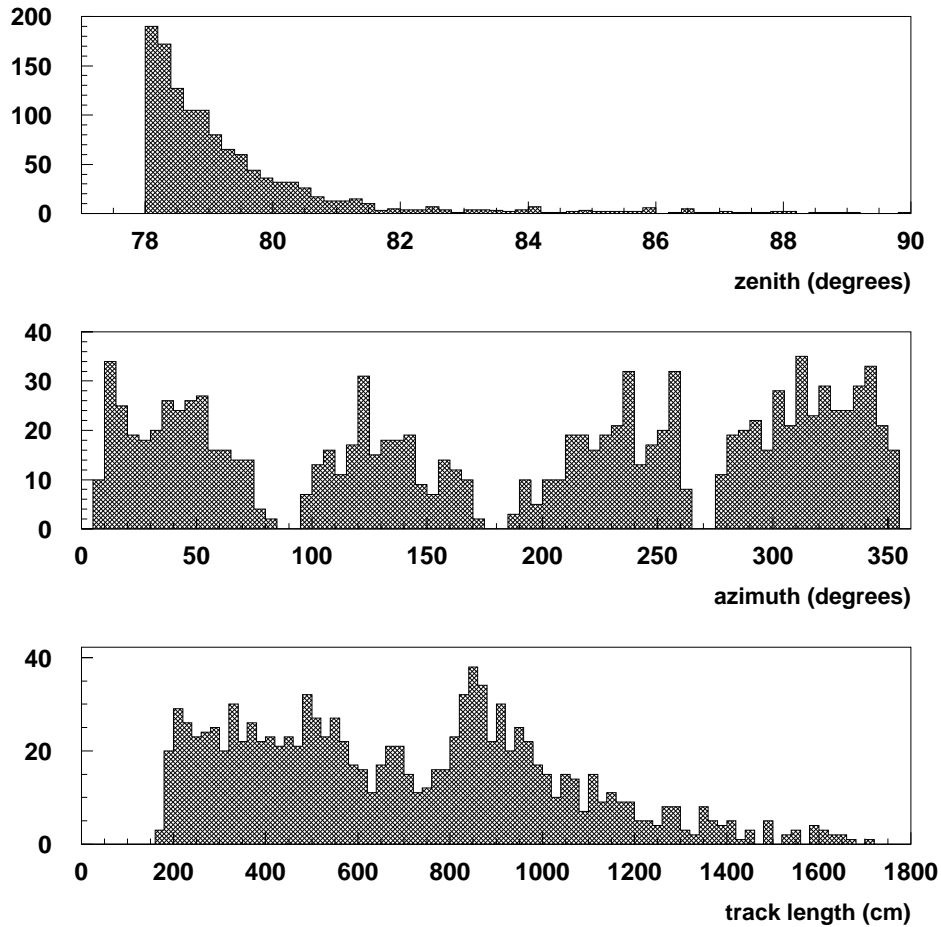
Figure 1. Zenith angle, azimuth and track length distributions for horizontal muons with a measured zenith angle greater than 78°.

Backgrounds could arise from high energy atmospheric muons with a range greater than 14 kmwe, or from muons which multiple scattered from a different zenith angle before reaching the detector. We calculated the first background to be 0.1 events, and ran a Monte Carlo which indicated the second background to be less than 0.5 events. We conclude that the expected background is less than one event.

The neutrino-induced muon flux Φ_μ, can be expressed as

$$\Phi_\mu = N_\mu / t \, A \, \Omega \, \varepsilon$$

where t is the time exposure of the detector in seconds, A is the area, Ω is the solid angle subtended by the detector in steradians, and ε is the detection efficiency for the muons in the detector.

The analyzed data spanned the period from April 14, 1992 to April 24, 2002. The exposure time was calculated from the start and end times of every processed data run. The calculated exposure for this analysis, including corrections for the detector duty cycle and electronics dead time during data taking, is 2.00×10^8 s. To estimate the effective area for this analysis, Monte Carlo muons were uniformly generated and the effective area for each track calculated. For zenith angles greater than 78° the average area was 90.6 m^2. For $\theta_z < 82°$ the average effective area was 86.7 ± 0.3 m^2. The solid angle was calculated from a Monte Carlo to be 1.77 sr. The trigger and reconstruction efficiency $\varepsilon = 0.53$.

Systematic errors arise with the uncertainty in the background of 0.7 events (1%), uncertainties in the scan efficiency (5.6%) and uncertainty in the energy distribution as it affects the efficiency of the 2° multiple scattering cut (5%). Adding these errors in quadrature, we assign an overall systematic uncertainty to the neutrino flux calculation of 7.6%.

The resulting neutrino-induced muon flux is

$$\Phi_{\nu\mu} = 3.99 \pm 0.47 \, (stat) \pm 0.29 \, (sys) \times 10^{-13} \, cm^{-2} sr^{-1} s^{-1}$$

Super-Kamiokande and others have analyzed atmospheric neutrino events and concluded that neutrino oscillations modify the zenith angle distribution of the ν_μ flavor component of the atmospheric neutrino flux. For a neutrino energy of 40 GeV and assuming $\Delta m^2 \sim 3.5 \times 10^{-3}$ eV^2 and maximal θ_{23} mixing, the probability of oscillation for a ν_μ from 82°, (L ~ 130 km) is 2.1×10^{-4} while for a ν_μ from 98° (L ~ 2000 km) it is 0.04. Our modest statistics and 90 - θ_z ambiguity make an oscillation analysis of these events impractical.

Several models for neutrino production in Active Galactic Nuclei predict large and potentially measurable fluxes of very high energy neutrinos. These neutrinos would then produce high energy muons with energies from a few TeV up to 100's of TeV. In this energy range the dominant energy loss process for the muons in iron is electron pair production,

followed by bremsstrahlung. Both processes produce large electromagnetic showers in the Soudan 2 detector which are easily detected and measured.

To understand the response of the tracking calorimeter to these TeV muons, a simulation was performed. High energy muons were propagated through the Soudan 2 detector and the amount of energy they deposited was calculated in a GEANT-based Monte Carlo. Three different muon energies were studied: 5, 20 and 100 TeV. We found that 60% of the 5 TeV muons lose 5 GeV or more, 91% of the 20 TeV muons and 99% of the 100 TeV muons lose at least 5 GeV in the detector.

The muons identified for the horizontal muon flux measurement were subjected to a predetermined cut of 5~GeV on the amount of energy loss they experienced in the detector. None of the 65 events had visible radiated energy loss greater than this cut.

Based upon the observation of zero events, together with our efficiencies, we calculate 90% CL upper limits for the integral muon flux above three energies, which are shown in Figure 2. Our limit is close to the highest predicted flux; however that flux is not ruled out. The limits are lower for higher energy cut-offs because of the higher probability of detecting a large energy loss. As another test for an extraterrestrial component in the horizontal muon events, we have
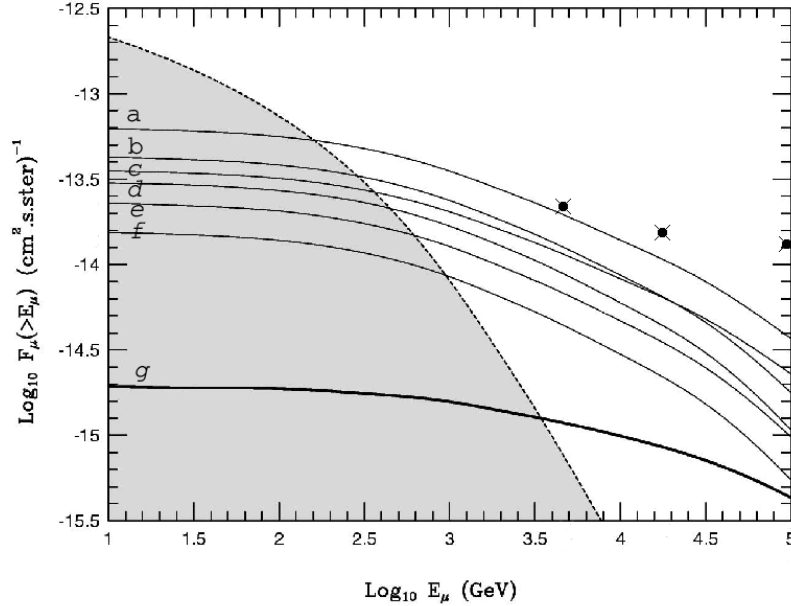
Figure 2. Our muon flux limits as a function of muon energy. Also shown are several model predictions of AGN fluxes. The shaded area is the atmospheric neutrino induced muon flux.

examined them for evidence of point sources. Figure 3 shows the directions of the 65 horizontal muons in galactic coordinates using an Aitoff projection of the galaxy. For each muon, the two possible directions are plotted. We observe that no clusters involving two or more muons within the detector's angular resolution $0.3° \times 0.3°$ appear within the plot.
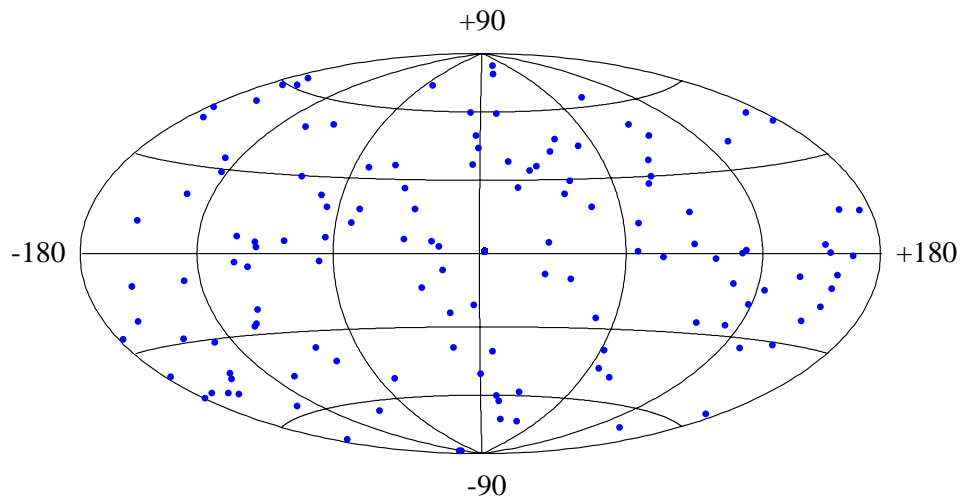
Figure 3. Aitoff projection of the 65 horizontal muon candidates. Each event has two projections due to the ambiguity in direction.

(M. C. Goodman)

I.A.5. ZEUS Detector at HERA

a) Physics Results

Six papers were published in this period and nine more manuscripts were submitted for publication. In the following, we shall summarize some of the published papers.

i) *Inclusive Jet Cross-sections in the Breit Frame in Neutral Current Deep Inelastic Scattering at HERA and Determination of α_S*

Inclusive Jet differential cross sections have been measured in neutral current deep inelastic e^+p scattering for boson virtualities $Q^2 > 125$ GeV^2. Jets were identified in the Breit frame using the longitudinally invariant k_T cluster algorithm. Measurements of differential inclusive jet cross sections were presented as functions of jet transverse energy in the Breit frame, jet pseudorapidity and Q^2. Next-to-leading order QCD calculations agree well with the measurements both at high Q^2 and high jet transverse momentum. Values of the strong coupling constant α_S have been determined in different bins of jet transverse momentum, see Figure 1. The running of the coupling constant is clearly observed. From an analysis of $d\sigma/dQ^2$ for $Q^2 > 500$ GeV^2, a value of the strong coupling constant, extrapolated to the scale of the Z boson mass, of

$$\alpha_S(M_Z) = 0.1212 \pm 0.0017 \text{ (stat.) } {}^{+0.0023}_{-0.0031} \text{ (syst.) } {}^{+0.0028}_{-0.0027} \text{ (theo.)}$$

is determined.
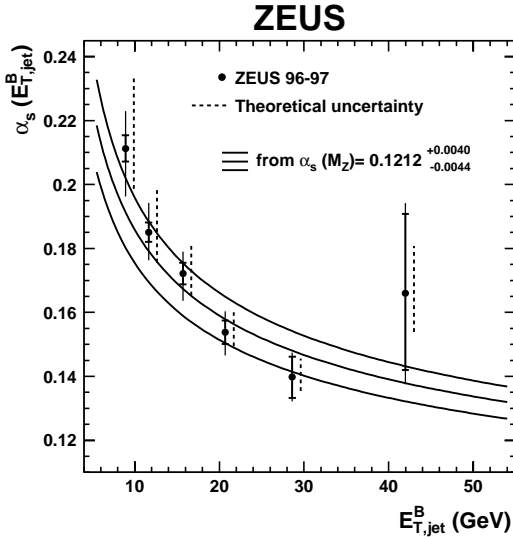
Figure 1. The $\alpha_S(\mu)$ values determined from the QCD fit of the measured differential jet cross sections versus jet transverse momentum. The three curves indicate the renormalization group predictions obtained from the $\alpha_S(M_Z)$ central value determined in this analysis and its associated uncertainty.

ii) *Measurement of the Q^2 and Energy Dependence of Diffractive Interactions at HERA*

Diffractive dissociation of virtual photons, $\gamma^*p \rightarrow Xp$, has been studied in ep interactions. The data cover photon virtualities $0.17 < Q^2 < 0.70$ GeV^2 and $3 < Q^2 < 80$ GeV^2 with $3 < M_X < 38$ GeV, where M_X is the mass of the hadronic final state. Diffractive events were selected by two methods: the first required the detection of the scattered proton in the ZEUS

leading proton spectrometer (LPS); the second was based on the distribution of M_X. The integrated luminosities of the low- and high-Q^2 samples used in the LPS-based analysis are 0.9 pb^{-1} and 3.3 pb^{-1}, respectively. The sample used for the M_X-based analysis corresponds to an integrated luminosity of 6.2 pb^{-1}. The dependence of the diffractive cross section on W, the virtual photon-proton center-of -mass energy, and on Q^2 is studied. In the low-Q^2 range, the energy dependence is compatible with Regge theory and is used to determine the intercept of the Pomeron trajectory. The W dependence of the diffractive cross section exhibits no significant change from the low-Q^2 to the high-Q^2 region, see Figure 2.

In the low-Q^2 range, little Q^2 dependence of the diffractive cross section is found, a significantly different behavior from the rapidly falling cross section measured for $Q^2 > 3$ GeV^2. The ratio of the diffractive to the virtual photon-proton total cross section has also been studied as a function of W and Q^2. Comparisons were made with a model based on perturbative QCD.
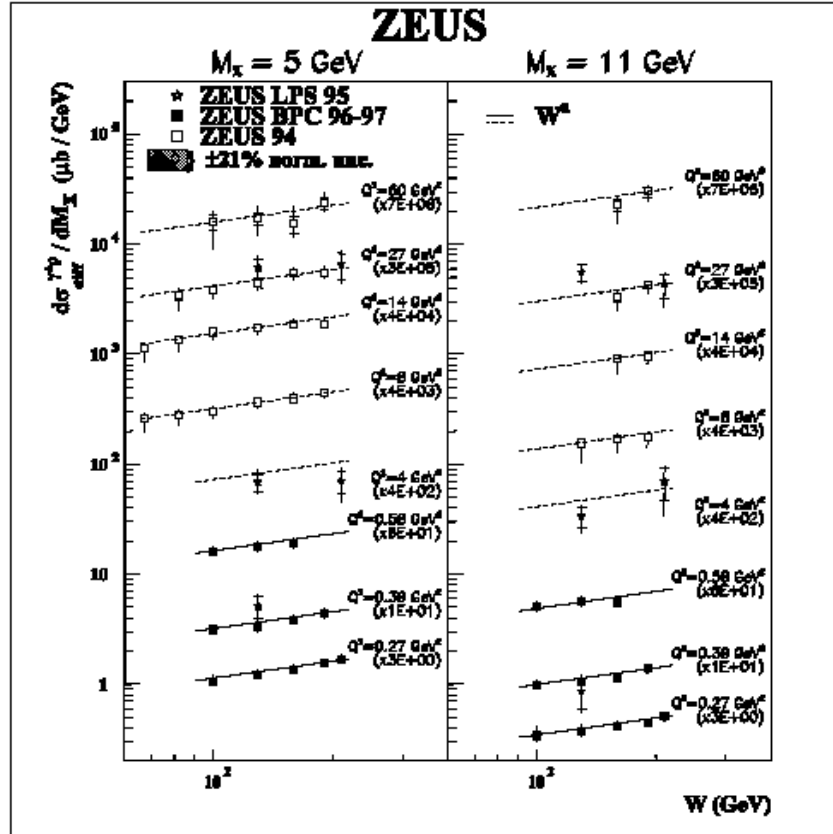
Figure 2. Diffractive cross sections for different Q^2 and M_X values as a function of W. The solid lines are the results of a fit to the form aW^b, which also gives a good representation of the higher-Q^2 data (dashed lines).

iii)   *Leading Neutron Production in e^+p Collisions at HERA*

The production of neutrons carrying at least 20% of the proton beam energy ($x_L > 0.2$) in e^+p collisions has been studied for a wide range of Q^2, from photoproduction to deep inelastic scattering. The neutron-tagged cross section, $ep \to e'Xn$, is measured relative to the inclusive cross section, $ep \to e'X$, thereby reducing the systematic uncertainties. For $x_L > 0.3$, the rate of neutrons in photoproduction is about half of that measured in hadroproduction, which constitutes a clear breaking of factorization. There is about 20% rise in the neutron rate between photoproduction and deep inelastic scattering, which may be attributed to absorptive rescattering in the γp system. For $0.64 < x_L < 0.82$, the rate of neutrons is almost independent of the Bjorken scaling variables x and Q^2. However, outside this range of x_L, there is a clear but weak dependence on these variables, thus demonstrating the breaking of limiting fragmentation. The neutron-tagged structure function rises at low values of x in a way similar to that of the inclusive structure function of the proton. The total $\gamma\pi$ cross section and the structure function of the pion have been determined using a one-pion-exchange model, up to uncertainties in the normalization due to the poorly understood pion flux. At fixed Q^2, the pion structure function has approximately the same x dependence as the inclusive structure function of the proton, see Figure 3.

iv)   *Measurement of Proton Dissociative Diffractive Photoproduction of Vector Mesons at Large Momentum Transfer at HERA*

Diffractive photoproduction of vector mesons, $\gamma p \to VY$, where Y is a proton-dissociative system, has been measured in e^+p interactions. The differential cross section, $d\sigma/dt$, is presented for $-t < 12$ GeV^2, where t is the square of the four-momentum transferred to the vector meson. The data span the range in photon-proton centre-of-mass energy, W, from 80 GeV to 120 GeV. The t distributions are well fit by a power law, $d\sigma/dt \propto (-t)^{-n}$. The slope of the Pomeron trajectory, measured from the W dependence of the ρ° and φ cross sections in bins of t, is consistent with zero. The decay-angle analysis for the ρ° and φ mesons indicates that the s-channel helicity conservation hypothesis does not hold, since both single and double helicity-flip contributions are observed. No available perturbative QCD calculation is able to describe this result quantitatively.
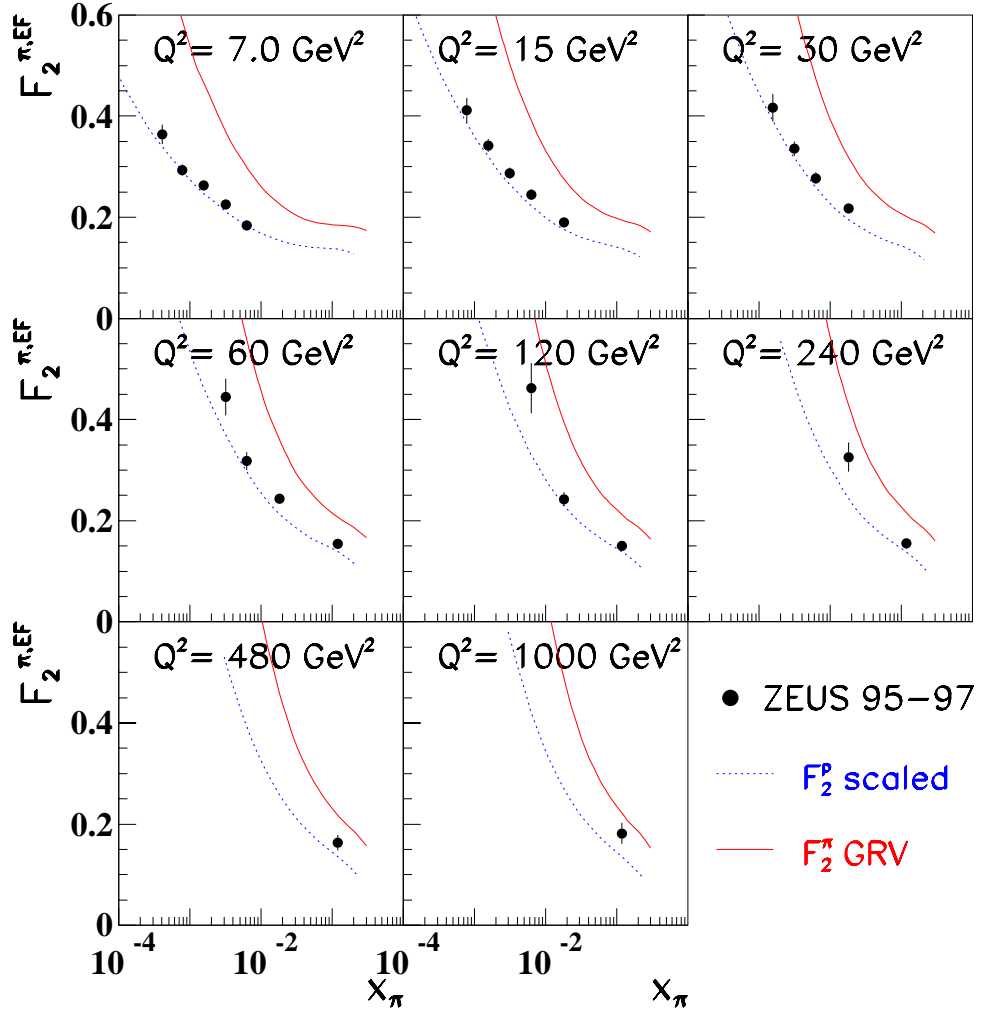
Figure 3. The pion structure function as a function of x_π in bins of Q^2 determined for $0.64 < x_L < 0.82$. The pion flux, used to determine the structure function, is the effective OPE flux used in hadron-hadron charge exchange reactions. The dotted lines indicate the proton structure function, scaled by 0.361. the solid curves are the pion structure function from the GRV parameterization.
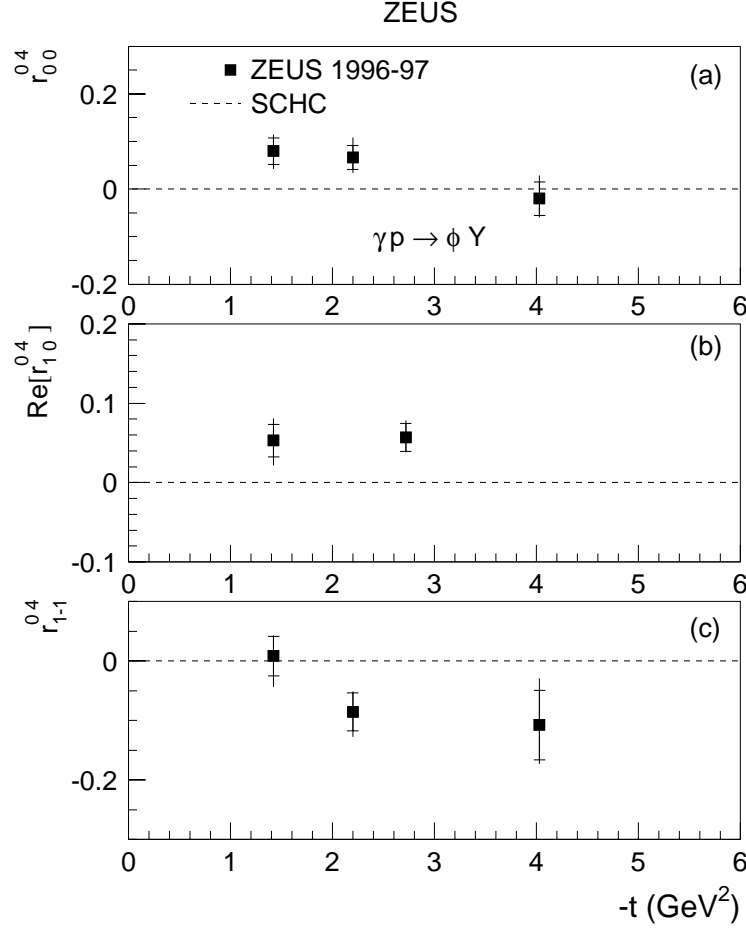
Figure 4. The fitted parameters of the decay-angle distributions for proton-dissociative φ meson photoproduction as a function of –t. The s-channel helicity conservation prediction is shown as the dashed lines.

b)   HERA and ZEUS Operations

The second half of 2002 was used to further investigate the reasons for the high machine backgrounds as observed by the colliding beam detectors and to provide some luminosity to the experiments. Three different backgrounds have been identified: positron-gas interactions, proton-gas interactions and synchrotron radiation. Currently the background rates are such that the tracking detectors can not be operated in the presence of larger positron or proton beam currents. The studies involve the tracking systems as well as the calorimeter. In addition, detailed Monte Carlo studies of the beam lines are used to redesign the set of collimators employed to reduce the rate of synchrotron radiation entering the detectors.

Despite the problems with the machine this period is being used to commission the newly installed tracking detectors, the Microvertex Silicon tracker and the Straw Tube Tracker in the

forward direction. Recently, several problems have surfaced with the operation of the Straw Tube Tracker, which will require a prolonged access to be mended.

(J. Repond)

I.B. EXPERIMENTS IN PLANNING OR CONSTRUCTION

I.B.1. The Endcap Electromagnetic Calorimeter for STAR

During the second half of 2002, the collaboration of ANL, Indiana University, and other institutions reached a major milestone with the installation of the support structure for the lower half of the endcap electromagnetic calorimeter on the poletip of the STAR magnet at Brookhaven National Lab. Two-thirds of this half was filled with the megatiles built at Indiana and shower-maximum detectors (SMD) built and tested at ANL. One member of the ANL group was at Brookhaven to install the SMD modules in the structure and to observe the installation of the structure on the poletip. Collisions at STAR were not established until the very end of the year, and commissioning of the detector will continue during a run scheduled to last until May 2003. Figure 1 shows the installation of the detector. Following this accomplishment, work began on the tasks needed for completion of the full calorimeter which, as previous reports have discussed, is crucial for the spin physics goals of the STAR experiment.

One of the ANL group's responsibilities is to test the finished modules with cosmic rays. Development of software and techniques for analysis of the test data was essentially completed by the end of the year. An analysis of the data indicates that systematic uncertainties may be as high as 10% due to effects such as drifting MAPMT gains, however gain variations from strip to strip are observed to be less than 10%. This figure does not include an apparent dependence on the length of the wavelength-shifting (WLS) fibers, an effect which is nearly identical in all modules. Our plan was to measure the relative gain of each strip to within 20%, and we have concluded that except for length effects, the gains of more than 98% of the strips are identical to within 10%. Of course we will continue to monitor the gains of the remaining modules. In addition, at the end of the year we repaired or replaced most of the clear fiber bundles used in our test stand to transport light from the WLS fibers to the MAPMTs because some fibers had been damaged and were transmitting less light. We expect that the replacement of these fibers will improve the quality of our test data and simplify the analysis.

The ANL group is making good progress toward the goal of having all SMD modules installed in the full detector during the shutdown scheduled for the summer of 2003. As of the end of the year, a total of 20 modules had been glued and 14 had been fully tested, including the 8 already installed at Brookhaven. We hope to have adequate time to build and fully test the remainder of the 24 modules needed for the full calorimeter before installing them during the shutdown.
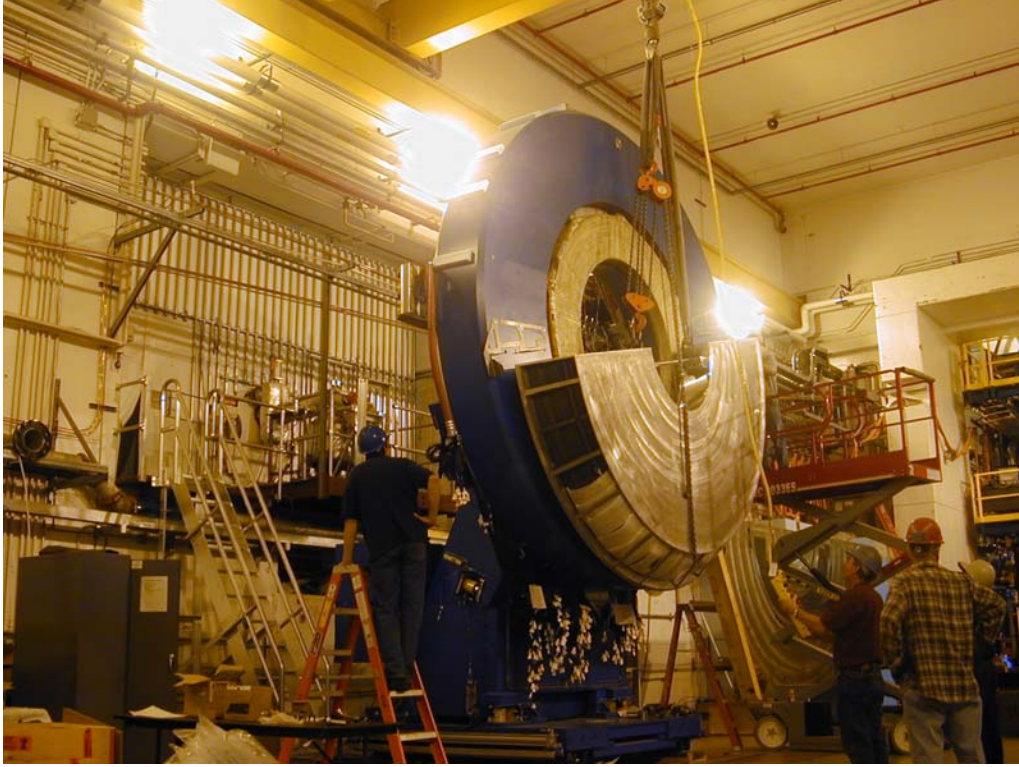
Figure 1: The lower half of the endcap electromagnetic calorimeter, with four of its six sectors filled with scintillators, is shown hanging from a crane as it is moved the final few inches into position on the STAR magnet poletip.

(R. V. Cadman)

I.B.2   MINOS - Main Injector Neutrino Oscillation Search

The phenomenon of neutrino oscillations allows the three flavors of neutrinos to mix as they travel through space or matter. The MINOS experiment will use a Fermilab muon neutrino beam to study neutrino oscillations with higher sensitivity than any previous experiment. MINOS is optimized to explore the region of neutrino oscillation parameter space (values of the Δm^2 and $\sin^2(2\theta)$ parameters) suggested by atmospheric neutrino experiments: IMB, Kamiokande, MACRO, Soudan 2 and Super-Kamiokande. The study of oscillations in this region with an accelerator-produced neutrino beam requires measurements of the beam after a very long flight path. This in turn requires a very intense neutrino beam (produced for the MINOS experiment by the Fermilab Main Injector accelerator) and massive detectors. The rates and characteristics of neutrino interactions are compared in a 980-ton "near" detector, close to the source of neutrinos at Fermilab, and a 5400-ton "far" detector, 735 km away in the underground laboratory at Soudan, Minnesota. The MINOS detectors are steel-scintillator sandwich calorimeters with toroidally magnetized 1-inch thick steel planes. The detectors use extruded plastic scintillator with fine transverse granularity (4-cm wide strips) to provide both calorimetry (energy deposition) and tracking (topology) information. The neutrino beam and

MINOS detectors are being constructed as part of the NuMI (Neutrinos at the Main Injector) Project at Fermilab.

Results from the Super-Kamiokande, Soudan 2 and MACRO experiments provide evidence that neutrino oscillations are taking place within the region of parameter space that MINOS was designed to explore. The best value of Δm^2, around $3 \times 10^{-3} eV^2$, has motivated the use of a lower energy beam for MINOS than was initially planned in order to improve sensitivity at low Δm^2. Argonne physicists and engineers are involved in several aspects of MINOS construction: scintillator-module factory engineering, near-detector scintillator-module fabrication, near-detector front-end electronics, near- and far-detector installation and the construction of neutrino beamline components.

Several important MINOS detector milestones were achieved during the second half of 2002. In July, the magnet coil for the first half of the far detector, Supermodule 1, was installed and energized. Since that time Supermodule 1 has been routinely recording cosmic-ray muon and atmospheric-neutrino data with the magnetic field turned on. Figure 1 shows the coil conductors emerging from the last plane of Supermodule 1 as it appeared during the underground lab dedication in July. In September, Argonne physicists and engineers led the successful CERN
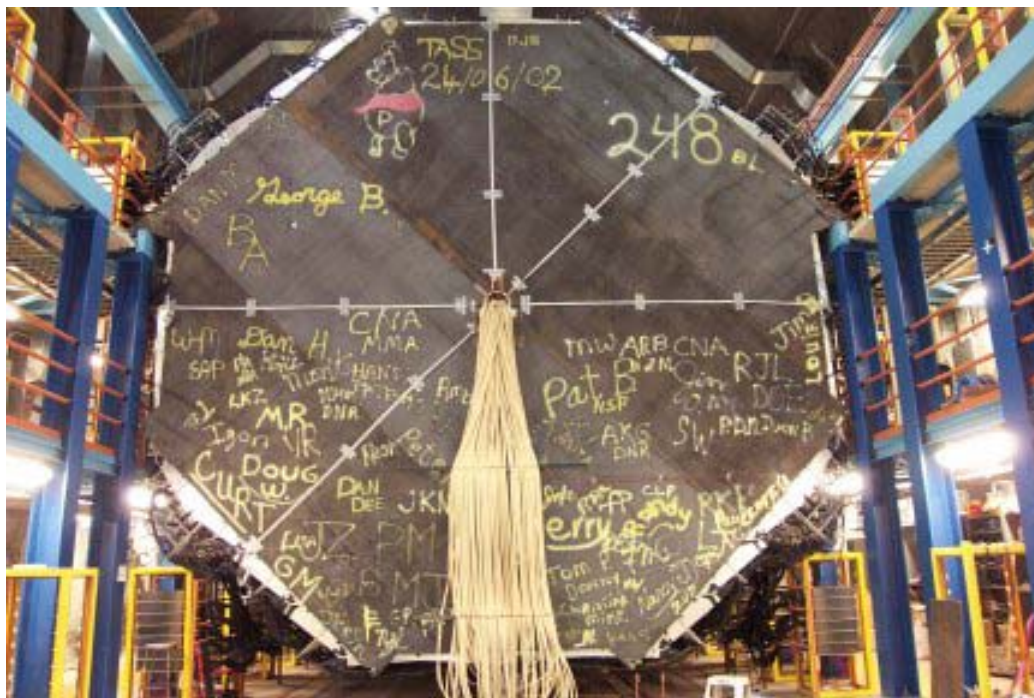
Figure 1. The completed magnet coil of Supermodule 1. A coil constructed of 180 turns of ordinary copper building wire is used to magnetize the steel planes of the first Supermodule. The photograph shows the coil conductors emerging from the water-cooled copper tube that has been threaded through the central hole of the steel-and-scintillator detector planes. The photograph was taken at the July 2, 2002 Grand Opening of the MINOS Far-detector Laboratory at Soudan, shortly before the first planes of Supermodule 2 were installed. The coil was energized at the end of the month and has been in routine operation for data taking since that time.

test-beam run of the Calibration Detector with near-detector front-end electronics. The production manufacturing of near- detector electronics began shortly thereafter. In November, the Argonne assembly facility for near-detector scintillator modules completed its work and was decommissioned. Figure 2 shows the factory staff with the final module.

Figure 2. The final MINOS near-detector scintillator module constructed at the Argonne assembly facility. The photo shows some of the Argonne factory staff that built, tested and delivered 573 near-detector modules that are now installed on steel planes at Fermilab. A number of spare modules were also constructed before the factory was decommissioned in December 2002. The assembled planes will be moved underground and installed in the near detector during the spring and summer of 2004.

The magnetization of the MINOS far detector gives it the capability of performing a unique atmospheric-neutrino measurement. The bending of charged particles in the magnetic field distinguishes positive from negative muons up to 70 GeV/c. This allows the detector to measure charged-current muon-neutrino and antineutrino interactions separately. A difference in the oscillation parameters of neutrinos and antineutrinos would constitute a violation of CPT symmetry, which could not have been observed in earlier experiments. In the spring of 2002 it was learned that the study of atmospheric neutrino events in MINOS data would require a veto shield to suppress backgrounds from downward going cosmic-ray muon interactions. A prototype shield was installed during the summer, using far-detector scintillator modules covering the top and sides of the detector to flag the presence of cosmic-ray muons in candidate neutrino events. An optimized shield covering Supermodule 1 was nearly completed by the end

of the year, so that the search for CPT violation in atmospheric neutrino events can begin in early 2003. A similar shield will be constructed over the remainder of the far detector when it is completed later in the year. Figure 3 shows the nearly completed shield over Supermodule 1 as well as the first few planes of Supermodule 2.

Figure 3. Photograph of the top of the MINOS far detector at Soudan. This August photo shows the nearly completed veto shield covering the top of Supermodule 1 and also the first few planes of Supermodule 2. The veto shield is used to flag the presence of cosmic ray tracks that can create a background to atmospheric neutrino events in the detector. A clean sample of muon-neutrino charged-current events is being used to search for any difference in the oscillations of atmospheric neutrino and antineutrino events, which would constitute a violation of CPT symmetry.

One major focus of work by the Argonne MINOS group is scintillator module construction. ("Modules" are subassemblies of 20 or 28 extruded plastic scintillator strips.) Scintillator module assembly for MINOS is taking place at assembly facilities at Argonne, Caltech and the University of Minnesota in Minneapolis. The Argonne group designed and built the assembly machines and tooling for all three module factories. Argonne physicists and engineers serve as NuMI Project WBS Level 3 Managers for the design and construction of the machines needed to construct scintillator modules and for the operation of the three factories.

In early 2001 the Argonne group commissioned the assembly facility for near detector modules in Building 369 at Argonne. The preparation of Building 369, which has air conditioning and more floor space than Building 366, was made possible by substantial financial assistance from the Laboratory administration. In November 2002 the group had completed the assembly of all 573 near detector modules, which were shipped to Fermilab to be installed on

steel detector planes. All near-detector planes had been assembled by the end of the year and were ready to be mounted on the detector when the underground laboratory is ready in 2004.

The second major focus of the Argonne MINOS group is electronics and data acquisition for the experiment. Argonne physicists and engineers continued to serve as the Level 2 manager for electronics and the Level 3 manager for the near-detector front-end electronics in 2002. The near detector must have fast front-end electronics with no dead time because of the high instantaneous rate of neutrino events at Fermilab. This is accomplished using a special MINOS modification of the Fermilab QIE ASIC chip. Most components of the near-detector front-end electronics, along with protocols for communication among the various boards, are the responsibility of the Argonne electronics group. The Argonne group also developed software to operate and study the performance of the readout electronics chain and performed simulations of electronics response.

Physicists and engineers from Argonne, Fermilab, IIT and the Rutherford Lab completed their certification of electronics performance in a "vertical slice test" at Argonne in early 2002. The group installed and commissioned a full system of front-end and data-acquisition electronics on the MINOS Calibration Detector (CalDet), which successfully recorded data in a CERN test beam in September 2002. The main goal of this run is to compare directly the responses of the near and far detector electronics, which were used to read out opposite ends of the same scintillator strips in the calorimeter. The CalDet system included enough near-detector front-end channels to read out all 128 pixels of two M64 near-detector photomultiplier tubes. The analysis of data recorded during this run was well under way at the end of the year.

As Argonne work on MINOS electronics, scintillator module fabrication and far detector installation ramped down during 2002, Argonne physicists began to shift their effort to more urgent tasks for the experiment. In December the physicist who had been co-manager for MINOS electronics since 1998 relinquished that position to serve as co-manager for MINOS near detector installation. Other Argonne physicists were able to devote more time to construction and testing of NuMI neutrino beam components at Fermilab. This work focused on neutrino-beam horn testing and magnetic field mapping, readout and integration of target hall instrumentation, and construction of the facility to repair highly radioactive beam components. Finally, Argonne physicists and engineers were able to devote time to the design of a next-generation experiment in the NuMI beamline. They were co-authors on a Letter of Intent, submitted to the Fermilab PAC in June 2002, to build a 20-kton detector to search for $\nu_\mu \rightarrow \nu_e$ oscillations several degrees off-axis in NuMI beam in Minnesota. The observation of such events would allow a measurement of the θ_{13} mass-mixing parameter, which could eventually lead to the construction of an even larger detector to search for CP violation effects in the NuMI beam.

(D.S. Ayres)

I.B.3   ATLAS Detector Research & Development

a)   Overview of ANL ATLAS Tile Calorimeter Activities

The TileCal subsystem continued making excellent progress in the second half of 2002. Module construction was completed with 65 modules being mechanically constructed. Module instrumentation has continued at a rate of 1 module per month and we are continuing to test (and repair where necessary) modules instrumented at MSU. 54 modules have been shipped to CERN. However, these were put on hold in October 2002 due to problems with obtaining sufficient storage space on the CERN site. We continue to routinely run the cesium source in all modules instrumented at MSU and replace tiles and repair fibers as needed. Argonne technical staff have made substantial contributions to the pre-assembly of the first extended barrel cylinder, which began in October 2002. A total of 12 modules were mounted by the end of the year. However, delivery of the support saddles has incurred significant delays and we do not expect to perform the load transfer from the assembly cradle to the saddles until February 2003.

(J. Proudfoot)

I.C.   DETECTOR DEVELOPMENT

I.C.1.   ATLAS Calorimeter Design and Construction

Mechanical construction of modules was completed in this period. The areas of ongoing work comprise: module instrumentation and testing; testbeam measurement of detector performance; engineering support of EBC pre-assembly at CERN; continued engineering evaluation of specific elements of the detector and final design of areas in the detector where special constraints must be accommodated. In addition, the engineering staff is now collaborating with Atlas Technical Coordination to specify and design components, which must be integrated with the calorimeter supports; in particular, the components associated with the moving system.

a)   Submodule Construction

The final submodule construction activity comprised the completion of the modifications to two submodules, which were cut to provide for the supports of the endcap liquid argon cryostat. All work in this area is now complete.

b)   Module Assembly

Module mechanical assembly is complete. A total of 64 standard length modules and one short module were constructed. The mechanical envelope of all modules meets the design

specification. Typically, the worst point on any module is out of plane by 0.5mm with the average deviation being approximately 0.25mm (Figure 1). The module assembly tooling is, however, being left in place until all modules have been safely delivered to CERN.
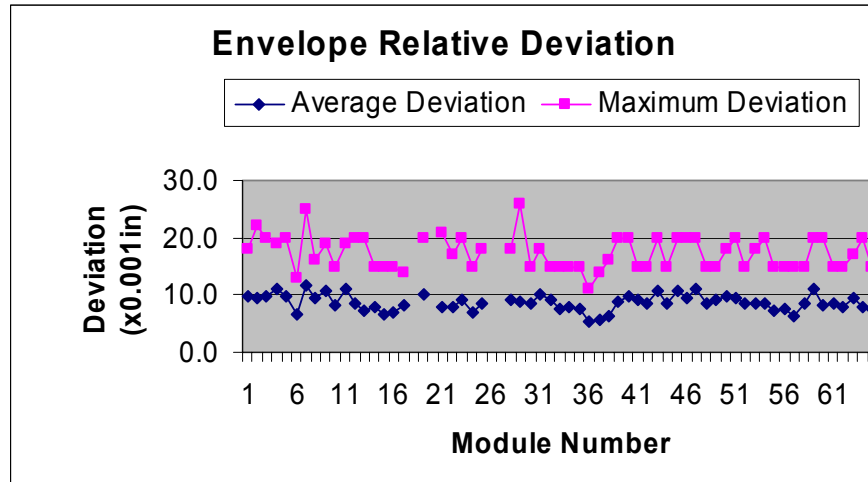
Figure 1. Module mechanical envelope – deviation from average surface

c)   Module Shipping

The shipping plan was changed in October 2002, when the CERN Tile Calorimeter group leader asked us to defer further shipments until they had located sufficient space for storage. At the close of 2002, 32 modules had been instrumented at MSU, of which 31 have been returned to Argonne. A total of 54 modules have now been sent to CERN. The delays in shipping modules to CERN will not be a problem for the preassembly schedule (the schedule for startup of EBA pre-assembly is Feb. 2004).

(J. Proudfoot)

d)   Instrumentation and Testing

Module instrumentation and testing is continuing routinely at a rate of approximately 1 module every 4 calendar weeks. The response uniformity continues to improve somewhat and we now regularly have an rms variation in response within a cell of less than 4%. Both modules 63 & 64 have been prepared for instrumentation and these will be instrumented concurrently in January 2003. This will complete the instrumentation work in the United States.
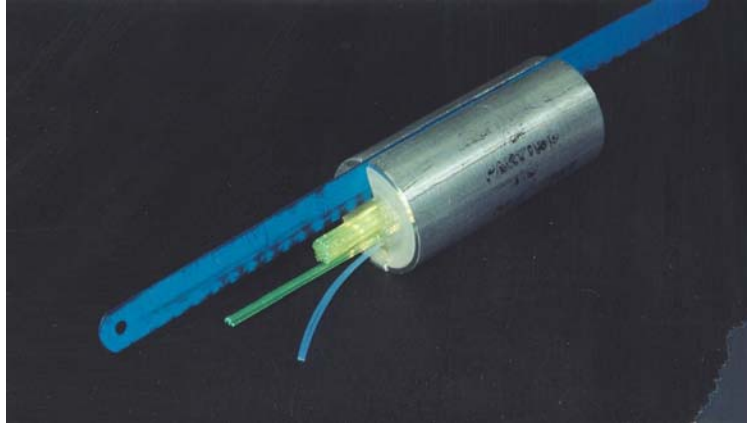
Figure 2. The approach developed for module repairs at CERN in the case that no pull-rods are available for the replacement of a defective fiber.

Several modules have been shipped to CERN, which have been identified as in need of rework to bring their uniformity of response up to a higher standard than originally specified by the Tile Calorimeter group. We have developed simple tools to allow us to carry out these repairs. In particular, many of the early modules do not have pull rods with which one could easily replace single fibers. We there developed a simple holder with which we could cut a saw-draft in the aspirin tube such that fibers glued in this location would view the corner of the photo-multiplier tube. This is shown in Figure 2 above. A technician was sent from Argonne to CERN for two weeks in November and completed repairs on 6 of the 12 modules in need of repair. The remaining repairs will be completed in early 2003.

(J. Proudfoot)

e)   Test Beam Program

Once again the testbeam program was very intensive. We did final calibration on three barrel modules and six extended barrel modules. These modules were selected as representing a variety of instrumentation techniques used in their construction. In addition, two periods of testbeam time not related to calibration were used. The first of these was a successful run combining detectors from the pixel group, the tile group and the muon group. The second of these used the testbeam and module infrastructure to diagnose irritating problems that would cause much concern in running ATLAS. This was the first of our so-called experts' week.

The testbeam program has been used for at least two purposes in the past: calibrate modules and discover problems. A very important problem was discovered this time in the testbeam. We found that the high voltage on many channels was not stable. The power supplies tripped on over current, and to recover operation for an entire drawer, it was necessary for us to destroy these particular PMT bases using higher current supplies. The problem was related to the manufacturer not cleaning solder flux sufficiently. After these tests, and tests in numerous collaboration labs across the world, a decision to clean all the PMT bases was made.

This year's testbeam results were very encouraging. The goal is to set the gains of each cell to 1.2 pC/GeV at the EM scale using only the Cs source. We expect this method to be reliable to 5%. The detectors are then checked with particles of all types and energies and in all cells to crosscheck. In 2001, we had a problem with the 20 GeV results, which indicated that something was incorrect at the ~10% level. All checks of the calibration constants indicated no apparent error. However, this year, elements in the beamline magnets were changed, and this spurious result went away. Looking at all the modules calibrated so far, we find that for all cells set with Cs, the average pC/GeV is 1.22 with an RMS value of 4.8%. These numbers give us good confidence that we can easily set the gains of any cell, under any conditions.
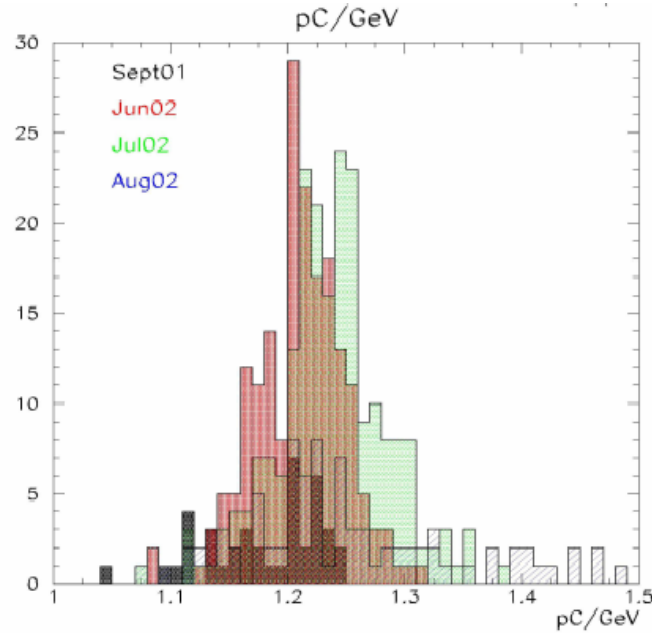
Figure 3. Cesium/Beam calibration reproducibility for 14 modules calibrated in the CERN testbeam.

As mentioned above, experts' week drew together experts in the collaboration from all areas of software and electronics. For years we have had annoying problems which, for the most part, could be cured by cycling the power supplies. These items were detailed and one by one addressed by the experts. Solutions were found in the software and bugs were found in the firmware. A large fraction of these problems were solved, but there are still some remaining that need further investigation, as shown in Table 1.

Problem	Solution
DAQ and Cs Cannot Run sequentially without power cycling	Generate ADC reset via TTC before DAQ run
Unstable CIS Settings in DAQ: DAC/CAP not changing	Generate ADC reset via TTC before DAQ run. This stops the ADC from any activity.
Cs hangs at end of Cs run	Shut down TTC CIS activity before Cs *Not 100% conclusive, so FIC reboot is last resort.*
Cs has trouble switching 3-in-1 cards	Shut down TTC CIS activity before Cs
Stuck Digitizer Values from certain digitizer boards	Not seen in October. Cycle Power still only solution.
No CAN Communication with 6 drawers	Remove 10m of cable, Replace EB-ADC, replace connector
MB times need to be set twice to work	Bug in Eprom, 3-in-1lib updated
Drawers send (junk) data with TTC Fiber unplugged.	Stockholm will investigate a solution. Rather to send NO data than junk data.
Some drawers – sometimes - can't change 3-in-1 cards	CAN ADC Reset? Cycle power last resort

Table 1. DAQ issues identified during the fall "experts week".

(R. Stanek)

f)   Engineering Design and Analysis

Argonne engineering staff have agreed to take responsibility for several of the engineering tasks associated with assembly of the calorimeter as a whole and its support system. These tasks include: engineering analysis in which V. Guarino is responsible for evaluation of stresses in the cylinder connecting elements, as well as of the deflections in the cylinder during pre-assembly.

The support saddles were the subject of engineering reviews in August and in November. They are now in production (the procurement having been placed by CERN). However, the vendor is behind schedule and we do not expect to take delivery until early 2003.

Several engineering calculations are in progress:

- FEA calculation of deflections and stresses during assembly.
- FEA models have been developed for the analysis of the connections in the barrel. Extraction and analysis of the data will be completed in 2003.
- There has been ongoing work to check the impact of changes in the cryostat supports, which were made in this period.

- FEA calculations have been carried out to estimate deflections and stresses in the calorimeter structure during pre-assembly. This work is ongoing and further evaluation of the data needed to validate the FEA analysis during pre-assembly of EBC will be carried out when the saddles have been mounted. A draft document describing the data needed to evaluate the FEA calculations has been written.

(J. Proudfoot and V. Guarino)

g) EBC Cylinder Pre-Assembly

Argonne technical have had substantial involvement in the pre-assembly of the first extended barrel cylinder (EBC), which began at CERN in October 2002. Initial evaluation of the survey data has indicated a precision of order 0.5mm on measurements of the module positions, which will define the limit of the comparison to the finite element calculations. Argonne technical staff is therefore evaluating options to measure relative deflections with greater accuracy. At the end of 2002, 12 modules had been mounted on the cradle at CERN. However, the pre-assembly schedule is likely to be delayed due to both schedule and technical problems with the saddles. The earliest delivery date is now the second week in January 2003.

h) Work in Collaboration with ATLAS Technical Coordination

Argonne engineering staff has now taken on new responsibilities in collaboration with ATLAS Technical Coordination for parts of the calorimeter and toroid magnet moving systems. Significant progress has been made on several of our assigned tasks:

- The design of the calorimeter X-guide is complete.
- The design for the toroid X-guide and moving system is complete.
- Analysis of the present conceptual design of the Z bracket is close to completion (Figures 4 & 5). A draft of the results was sent to ATLAS TC in early November.
- A conceptual design and evaluation of the requirements on the moving control system has been completed. The layout of the moving test has been completed and parts are being collected and assembled. We expect that the first test will be carried out in November.

ITEM NO.	QTY.	PART	MASS [kg]
1	1	EB_Z_Brack4_A_Side	30
2	1	EB_Z_Brack4_A_SideL	30
3	1	EB_Z_Brack4_A_Top	29
4	8	M16_HCS	
7	1	connection	12
8	1	Connect_Pin	
10	4	McGill_5_8	
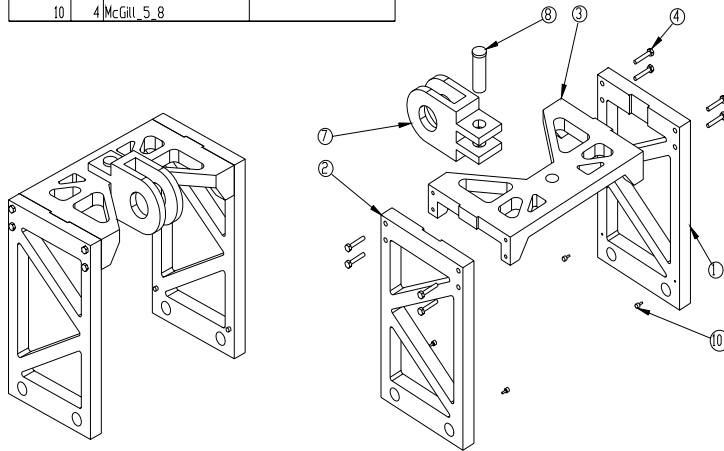
Figure 4. Design layout of the Z-bracket. This device mounts on the Atlas main rails and provides the connection to the hydraulic cylinder being used to move the detectors on the rails.
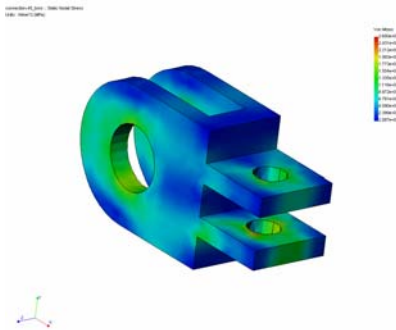
Figure 5. Results of a FEA calculation of stresses in the bearing used to connect the hydraulic cylinder to the Z-bracket.00

(J. Proudfoot and J. Grudzinski)

35

I.C.2. ATLAS Computing

Argonne (through David Malon) continued to lead the ATLAS-wide database effort in the 2nd half of 2002. In late 2001, triggered by a similar decision by CMS and the ATLAS policy to use common tools, ATLAS decided to move away from Objectivity/DB and towards a new common persistence tool called POOL, under the aegis of the LHC Computing Grid Project. The implementation of this decision formed a major direction of ANL effort over this reporting cycle. Dependencies upon the commercial database product Objectivity/DB were removed from ATLAS software releases in final quarter of 2002, as an orderly transition from Objectivity/DB to POOL as the ATLAS baseline persistence technology continued.

The U.S. ATLAS database group, also led by David Malon, delivered the first release of collection services for POOL. This release supports creation of and iteration over explicit collections instantiated in a relational database, with references pointing to data residing in a ROOT-file-based storage layer. Collections are queryable and filterable via SQL queries on associated metadata. The work was included in the POOL end-of-year release 0.3.0.

The U.S. group also assumed responsibility for management of MySQL and mysql++ packages for the POOL project, as well as for configuring and managing MySQL servers for both ATLAS and LCG. At an October database workshop in Orsay, the U.S. team organized (and now leads, through Sasha Vaniachine) a small group of people with MySQL database administration experience, charged with identifying long-term requirements and near-term strategies for deployment of relational database services for LHC. An outcome of this effort was a proposal for a multi-tier deployment model, presented to an LHC-wide audience at CERN in November.

Data Challenge 1 (the successor to Data Challenge 0, with roughly ten times the scale) began in this half-year. As with DC0, the ANL group provided database support for this major ATLAS effort. In particular, the ANL group was able to solve the unanticipated problem that at times we were being paced by physicist's ability to submit jobs instead of the available computational power. The ANL-provided solution was to apply the concepts of "virtual data" (the fundamental idea is that the recipe for creating data can often serve as a proxy for the data itself) to the job submission process. While virtual data concepts had been prototyped earlier, this was the first time they were used in ATLAS in a large-scale way. Their application allowed DC1 to stay largely on schedule. In addition to supporting ATLAS Data Challenge 1 production, the U.S. ATLAS database group delivered infrastructure and support for demonstrations at the Supercomputing 2002 conference in Baltimore, including demonstrations of EDG (European Datagrid) and U.S. grid interoperability, of virtual data, and of portal-based job submission and monitoring.

A meeting was organized at CERN in December to discuss coordination of database activities between online, offline, and ATLAS Technical Coordination. A workshop along these

lines, with a principal focus on conditions and other time-varying data, will be held at CERN in February 2003.

Tom LeCompte produced a prototype Tile Calorimeter calibration structure and successfully installed it in the TileCal reconstruction code. The structure for applying time-varying conditions data is present, although Athena does not presently support this, so the program uses ASCII files to select between different cable maps. Once Athena does support this (early 3Q03), the software will be developed further to use this provided functionality. Until then, the present scheme is being extended to include calibration gains and offsets.

(T. LeCompte)

I.C.3. Linear Collider

A group of physicist from the division has initiated an effort to develop the design of the hadron calorimeter (HCAL) for the Linear Collider. The aim is to develop a detector with a jet energy resolution of $30\%/\sqrt{E}$ or better. This type of resolution is necessary to properly disentangle different Higgs mechanisms responsible for the generation of massive particles.

Up to date, the best jet energy resolution, of the order of $50\%/\sqrt{E}$, has been obtained by the ZEUS experiment. A novel approach, named Energy Flow Algorithms (EFAs), is being evaluated to improve this performance further and possibly reach $30\%/\sqrt{E}$. EFAs utilize both the tracking and the calorimeter information to measure the energy of hadronic jets. Their optimal performance requires a calorimeter with extremely fine segmentation, of the order of 1 cm^2 laterally and layer-by-layer longitudinally. This fine segmentation leads to the order of 50 million readout channels for the entire HCAL. A traditional analog readout of this large number of channels would be prohibitively expensive, leading us to consider a simple digital readout. The favored technology choice for the active medium for this type of calorimeter uses Resistive Plate Chambers (RPCs).

The group works on the Monte Carlo simulation of the response of various detector designs with the goal of developing a set of complete Energy Flow Algorithms. First versions of a track - calorimeter cluster matching algorithm and of a photon identifier have been released. Results on single particle energy resolutions with analog and digital readout have been presented at various Linear Collider meetings.

On the hardware side, three RPCs have been built at Argonne and have been thoroughly tested with sources and cosmic rays. The chambers are 20×20 cm^2 in area and feature two gas gaps of 0.64 mm each. All three chambers were tested with a single pick-up pad of approximately 100 cm^2 and performed very well. Figure 1 shows the measured efficiency, fraction of streamers and noise rate as a function of the applied high voltage.
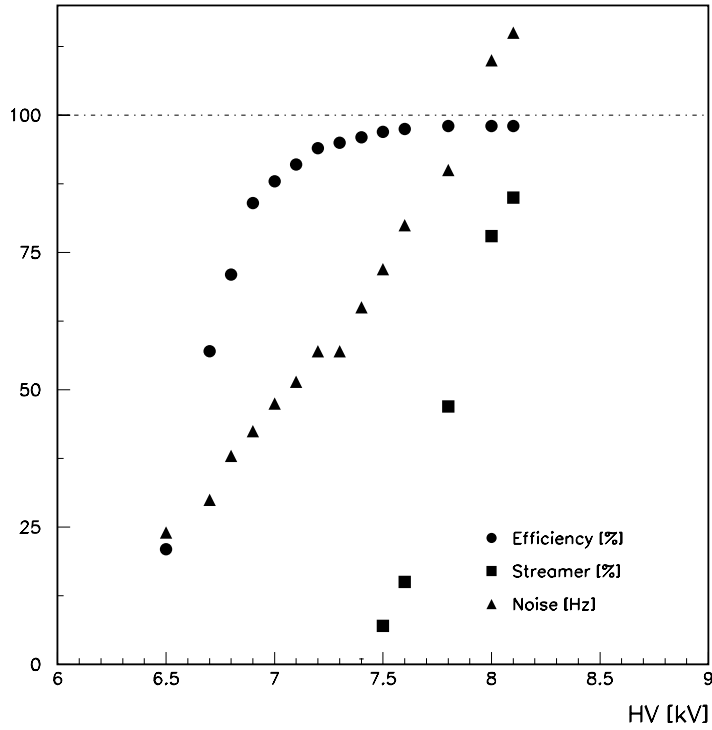
Figure 1. Efficiency, fraction of streamers and noise rate as measured with one of the chambers built at Argonne.

A conceptual design of the readout electronics has been developed. The system consists of four parts: a front-end ASIC located on the chamber, a data concentrator, a data collector and a trigger system. The front-end ASIC consists of an analog and a digital part. The analog part receives the input signals from 64 pads and contains shapers, pre-amplifiers and discriminators. The digital part can operate in two modes: in a trigger-less operational mode the channel number together with a time stamp are written to a buffer; in a triggered operational mode the writing and reading of the hit patterns to and from an intermediate buffer is controlled by an external trigger. Figure 2 shows the conceptual design of the digital part of the ASIC.
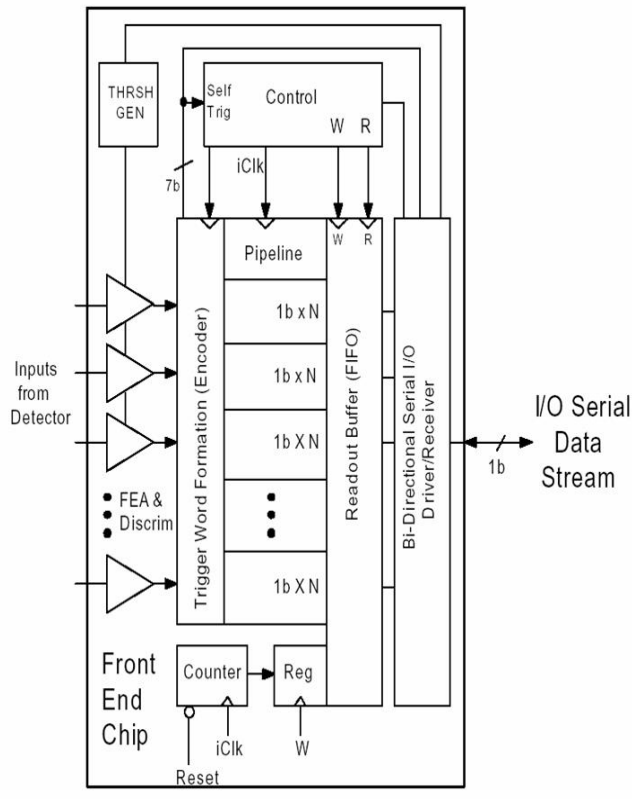
Figure 2. Conceptual design of the digital part of the front-end ASIC for the electronic readout of the chambers.

<div align="right">

(J. Repond)

</div>

I.C.4.   Electronics Support Group

CDF: We participated in building front-end electronics for the CDF Shower Max Detector at Fermilab, as part of the CDF Upgrade for Run IIA. We had major responsibilities for the electronics engineering of the system, including the coordination of the design engineering and system integration for the entire system, overseeing the production of all components, and ensuring that the overall system meets performance requirements. One member of our group was the Project Engineer for the electronics.   The system has 20,000 channels of low-noise electronics, and services two detector subsystems.   The development work was a collaborative effort between Argonne and Fermilab.

The production work for the electronics was completed in the spring of 2001.   All electronics were installed on the detector and commissioned for operation. We were successful in meeting the schedule goals in getting ready for Fermilab Run II, which is now in progress. To date, the system has performed well, with no major problems. In this period, we continued our participation with the experiment by providing technical support for the maintenance and repair

of all of the electronics for this subsystem. This includes those projects that were designed and produced by Fermilab personnel. We anticipate providing this support through the life of the experiment. The system includes 100 VME read-out boards called SMXR Modules, 600 front-end boards called SMD Modules, 6000 front-end daughter cards called SQUIDs, 100 front-end crate controllers called SMC Modules, 600 preamp boards, 15,000 preamp SIPS (Single In-line Package), and 60 crate monitor boards.

In addition to the Shower Max front-end electronics, we also built electronics for the CDF Level 2 Trigger. One project is called RECES. The modules in this subsystem receive trigger information from the Shower Max front-end electronics, and provide information to the Level 2 Trigger. This project has been completed, with all electronics installed and working. We also provide technical support and maintenance for this project.

Another project for the Level 2 Trigger System is the Isolated Photon Trigger. This subsystem receives information from the calorimeter, and triggers on isolated photons in the detector. The subsystem consists of three types of modules. This project is also completely installed and functional. Like the other projects, we provide long-term support and maintenance.

There are several upgrades being planned for the detector for Run IIB, the second part of Run II. One of these is the replacement of the Central Preradiator Chambers (CPR). They currently are wire chambers, similar in construction and performance to the Shower Max detector. The plan is to replace them with scintillator and phototubes. We are working with division physicists who are involved with this project, to provide support for interfacing the new detector to the existing front-end electronics.

ATLAS: We have major responsibilities in the development of electronics for the Level 2 Trigger of the ATLAS Detector at CERN. Working with colleagues from Michigan State University, we are responsible for the development of two parts of this system: the Level 2 Trigger Supervisor, and the Region of Interest (ROI) Builder.

The ROI Builder is the interface between the first level trigger and the second level trigger. When an event occurs in the detector, signals are sent from the front-end electronics to the Level 1 Trigger. The Level 1 Trigger collects event fragments from the front-end electronics over the entire detector, and stores them in a Readout Buffer. It evaluates the data, and identifies regions of the detector that could have an interesting event. The Level 1 Trigger boards then sends a list of addresses called pointers to the ROI Builder, identifying where the event data from the "Region of Interest," can be found. The ROI Builder collects the pointers for the event, and "builds" the event using the pointer list. It then sends the result to the Trigger Supervisor for distribution to Level 2 processors. The selected Level 2 Processor then executes algorithms using the pointers, and can request information to be sent from the Readout Buffers as needed. The ROI Builder is highly complex, using fast, high-density Field programmable Gate Arrays (FPGAs) to implement the functionality.

We have a working system at CERN, called the ATLAS Test Bed, where system tests are being performed. In the early part of 2001, the prototype ROI Builder was used in integration tests for different detector subsystems. The tests were largely successful. In this period, testing continued on the prototype system. We are providing much of the software development and support for this phase of the project.

Development efforts for the ROI Builder continued during his period. In the fall of 2001, we built a card called the Gigabit Ethernet Link Source card. This card receives information from the front-end electronics, buffers it, and then sends it to the ROI Builder using Gigabit Ethernet protocol. The cards make extensive use of large programmable logic arrays. They also have a large, fast synchronous memory that might allow their use as an intermediate data storage element. Testing of the prototype occurred at Argonne and at CERN in the winter of 2001-2002. The tests were highly successful. In February 2002, the ROI Builder was reviewed by an internal ATLAS review committee. The merits of using the Link Source card as a front end to the ROI Builder were discussed. While the general features were deemed acceptable, there were certain issues identified associated with error reporting and data slow control. We are now working on a design that incorporates these features. We expect to build the next version in 2003.

MINOS: We are involved with the development of electronics for MINOS, the Neutrino Oscillation Experiment at Fermilab and the Soudan mine. We have major responsibilities for the design, development, and production of electronics Near Detector, one of the two major detectors for this experiment. One member of our group is the Level 3 Manager for the Near Detector Electronics.

The heart of the front-end electronics for the Near Detector is a custom integrated circuit designed at Fermilab, called the QIE. The QIE digitizes continuously at 53 MHz. The operations are pipelined so that there is no deadtime due to digitization. The digitized data will be stored in a local memory during the entire period of the beam spill. The data will be sent from the local memory to a read-out board after the spill is over. In between spills, the electronics will record data from cosmic rays.

The QIEs and associated circuitry will be built on small daughter boards called MENU Modules, which resemble memory SIMMs. The boards contain a high density of surface mount parts. The MENU Modules plug in to a motherboard called the MINDER Module. The MINDERs reside in front end crates called MINDER Crates, which are a semi-custom design. There is a crate controller in the MINDER Crates called the KEEPER, which controls all activity in the crate. When data is acquired, it is stored on the MENU Modules. After data is acquired, the MINDER then initiates a readout operation, where the data is sent from the MENUs to a VME readout board, called the MASTER Module. The MASTER resides in a 9U VME crate located some distance away from the MINDER Crates. All of the board designs contain a high level of programmable logic to do the complex processing of data and control of operations.

The chip design, and the development of the QIE daughter board, are responsibilities of Fermilab. Argonne is responsible for the design the MASTER Module, the MINDER Module, the KEEPER, and the MINDER Crate. We also have overall responsibility for the design of the rest of the system for the Near Detector, including the specifications for the QIE performance. This is a major design and production project for our group.

In the spring of 2002, we staged a small production of 200 read-out channels, to be used in a test beam at CERN. This included the production of 200 MENU Modules, 20 MINDERs, 4 MASTERs, 4 KEEPERs, and timing modules. The system was first tested in the Vertical Slice test stand at Argonne, and included tests with photomultiplier tubes. As part of this effort, significant work was done on developing the data acquisition program and calibration routines. In this period, we shipped the electronics to CERN, and traveled there to participate in the installation and commissioning of the system. The test beam run was highly successful. Many good data runs were obtained, and on-line analysis of the data has yielded good results. Off-line analysis of the data is currently in progress. This was an important milestone for the project, and demonstrated that the new system could meet design performance in a high-rate beam environment.

We are currently completing the final review and sign-off of all system components. We are beginning production in January of 2003. Our next milestone is to produce 1600 channels of electronics for another test beam run at CERN, in the fall of 2003. Installation of electronics on the detector at Fermilab is scheduled to begin in the spring of 2004.

ZEUS: We were involved with the development of front-end electronics for the new Straw Tube Tracker Detector of the ZEUS experiment at DESY. The front-end electronics is situated directly on the detector. It uses a custom integrated circuit designed at PENN, called the ASDQ. The device receives charge pulses from the detector, and sends a digital signal to the "back end" electronics located off the detector in a counting room, where a timestamp for the signal is recorded. The back end processors then use the timestamps to reconstruct the trajectory of the particle through the tracking detector. There are ~12,000 channels in the detector in total, although the front end electronics multiplexes 6 detector channels into each readout channel to reduce the number of signal wires between the front end and the back end.

The production and installation of 200 electronics boards was completed in the spring of 2001. In the time since, significant experience was obtained in operating the detector and electronics, and two problems have emerged. One problem is that the fuses on the front-end boards are blowing, despite the fact that they are sized with a factor of two above nominal operating conditions. The other problem is that the digital signals produced on the front- end boards are radiating noise into other detector components. In this period, we have been studying both problems at the test bench at Argonne. We have designed fixes for both problems, and have made a proposal to retrofit the front-end boards during the next shut down. In November, we

participated in a review of our proposal. The proposal was largely accepted, with a few modifications suggested by the review committee. We are currently in the process of building small circuit boards that are part of the repairs. The boards will be installed on the detector at the next shut down, which is scheduled for March of 2003. We will travel to DESY at this time, to participate in the detector removal, installation of electronics, and re-installation of the detector.

(G. Drake)

II. THEORETICAL PHYSICS PROGRAM

II.A. THEORY

II.A.1. Differential Cross Section for Higgs Boson Production Including All-Orders Soft Gluon Resummation

The search for the Higgs boson is a central motivation for the experimental programs at the Fermilab Tevatron and the CERN Large Hadron Collider (LHC), with detection techniques guided by theoretical expectations about its production dynamics and decay properties. Precise theoretical calculations of the expected differential cross sections for production of the signal and backgrounds are important for quantitative evaluation of the required measurement accuracies and detector performance. Good estimations of the expected transverse momentum distributions can suggest selections in this variable that should improve background rejection.

Ed Berger (Argonne) and Jianwei Qiu (Iowa State University) completed a major calculation of the transverse momentum Q_T distribution for inclusive Higgs boson production at the energy of the LHC, $\sqrt{S}$ =14 TeV. Their work is reported in Argonne report ANL-HEP-PR-02-057 [hep-ph/0210135], published in Phys. Rev. **D67**, 034026 (2003). They concentrate on the behavior of the distribution in the region of small and intermediate values of Q_T where the cross section is large. They focus on the gluon-gluon partonic subprocess in perturbative quantum chromodynamics (QCD) $gg \rightarrow hX$ that dominates Higgs boson production in hadronic reactions when the Higgs boson mass is in the expected range $m_h < 200$ GeV. Using an impact-parameter b-space formalism, they employ all-orders resummation to master the large logarithmic coefficients that appear in finite-order perturbative expansions of the cross section in the strong coupling strength α_S. Their resummed results merge smoothly at large Q_T with the fixed-order expectations in perturbative quantum chromodynamics, as they should, with no need for a matching procedure. In their formulation, the Q_T distribution at LHC energies is entirely insensitive to the functional form employed for the non-perturbative input at large b, so long as the form used for this extrapolation does not modify the perturbative b-space distribution at small b.

Berger and Qiu provide distributions $d\sigma/dy\,dQ_T$ for Higgs boson masses from M_Z to 200 GeV. They also provide analogous results for Z boson production. Two points are evident in the comparison of Z boson and Higgs boson production, with $m_h = M_Z$. The peak in the Q_T distribution occurs at a smaller value of Q_T for Z production (4.8 GeV *vs.* 10 GeV), and the distribution is narrower for Z production. The larger QCD color factors produce more gluonic showering in the glue-glue scattering subprocess that dominates inclusive Higgs boson production than in the fermionic subprocesses relevant for Z production. After all-orders resummation, the enhanced showering suppresses the large-b (small Q_T) region more effectively for Higgs boson production.

Berger and Qiu compare the predicted Q_T distributions for Higgs boson production at different masses. The peak of the distribution shifts to greater Q_T as m_h grows, in approximately linear fashion, and the distribution broadens somewhat. As illustrated in Fig. 1, the mean value $<Q_T>$ grows from about 35 GeV at $m_h = M_Z$ to about 54 GeV at $m_h = 200$ GeV, and the root-mean-square grows from about 59 GeV to about 87 GeV. For Z production, they find $<Q_T> = 25$ GeV and $<Q_T^2>^{1/2} = 38$ GeV. The harder Q_T spectrum suggests that the signal to background ratio can be enhanced if Higgs bosons are selected with large Q_T.
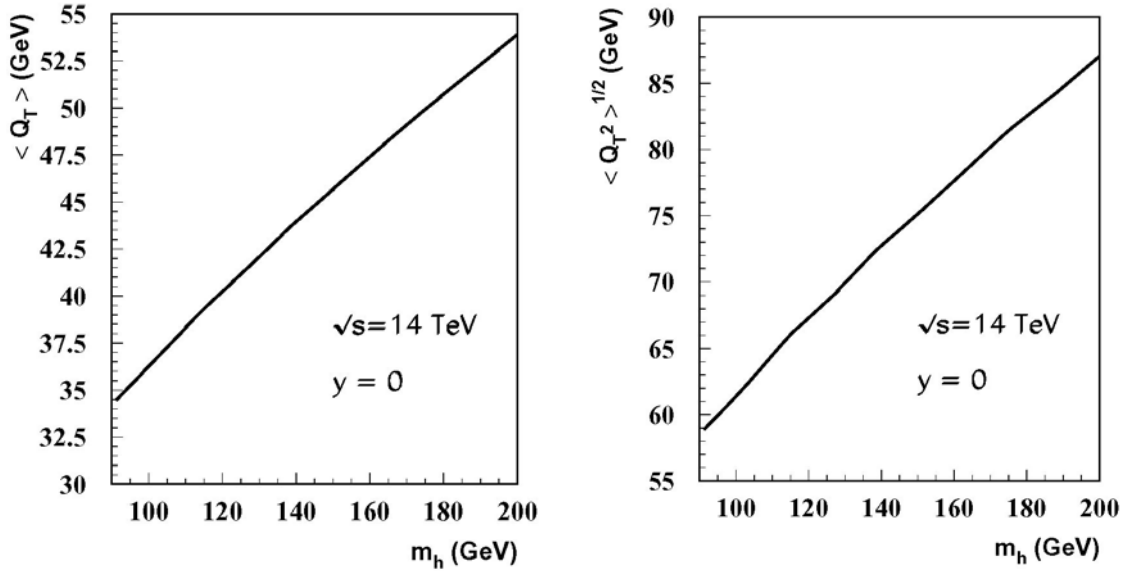
Figure 1. Predictions by Berger and Qiu of (a) the average value of the transverse momentum and (b) the root-mean-square for Higgs boson production as a function of Higgs boson mass at $\sqrt{S} = 14$ TeV and fixed rapidity y=0. Results are shown for Higgs boson masses m_h from M_Z to 200 GeV.

Research is continuing on the topic of Higgs boson production, and predictions appropriate for the physics program of the Fermilab Tevaton collider will be discussed in a future semi-annual report.

Berger was invited to present two seminars about this research at CERN, Geneva, Switzerland, in November, 2002; one a theoretical seminar in the Theory Division and another for the CMS LHC Collaboration. He spoke also about the results at the Illinois Institute of Technology, Chicago, November, 2002.

(E. L. Berger)

II.A.2. Associated Production of Gauginos and Gluinos

Edmond Berger (Argonne), Michael Klasen (Hamburg, Germany), and Tim Tait (Fermilab) updated their previous predictions [Phys. Rev. **D62**, 095014 (2000)] of the cross sections for associated production of gauginos and gluinos, providing results for the current Fermilab Tevatron energy $\sqrt{S}$ =1.96 TeV, and using the CTEQ6 parton densities. Their work is carried out at next-to-leading order in perturbative chromodynamics. The new results are reported in ANL-HEP-PR-02-123 [hep-ph/0212306] and published in Phys. Rev. **D67**, 099901 (2003). In Fig. 1, the predicted total cross sections for all six gluino-gaugino channels are shown as functions of the mass of the gluino (left) and as functions of the supersymmetry (SUGRA) parameter $m_{1/2}$ (right), for a gluino with mass 30 GeV.

The new paper also includes minor corrections to a few of the equations in the earlier publication.
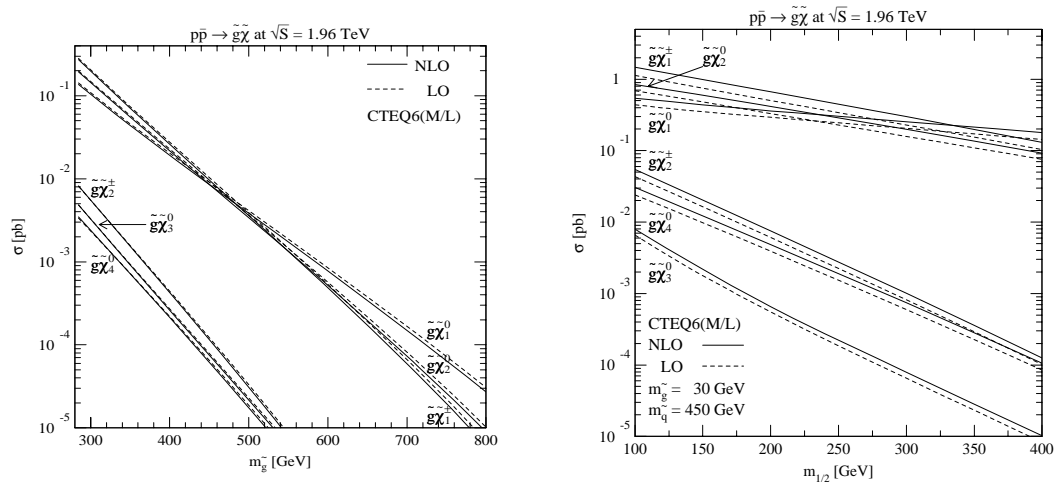
Figure 1. Predicted total cross sections at the Tevatron with total center-of-mass energy $\sqrt{S}$ =1.96 TeV for all six gluino-gaugino channels.

(E.L. Berger)

45

II.A.3. Phenomenology of Light Bottom Squarks

In Argonne report ANL-HEP-CP-02-085 [hep-ph/0209374], published in the Proceedings of the 31st International Conference on High Energy Physics, Amsterdam, July, 2002, Ed Berger summarizes the proposal that light bottom squarks and light gluinos are produced in reactions at current hadron collider energies and are responsible for the observed excess rate of bottom quark production above predictions of standard next-to-leading order perturbative quantum chromodynamics. The existence of bottom squarks with relatively small mass, similar to the bottom quark mass, was suggested earlier in Phys. Rev. Lett. **86**, 4231-4234 (2001) by Berger, Harris, Kaplan, Sullivan, Tait, and Wagner. This work has since garnered over 50 citations.

In his Amsterdam paper, Berger discusses contraints on the masses and couplings of light gluinos and light bottom squarks placed by data from hadronic and electron-positron reactions at various energies. He also summarizes the implications and consequences of the hypothesis, including production of pairs of like-sign charged *B* mesons at hadron colliders, an apparent increase in the rate of neutral *B* meson mixing at hadron colliders, changes in the hadronic widths of Upsilon states (observable with high-statistics samples of data from CLEO, BaBar, and BELLE), predictions for rare hadronic and radiative decays of the Upsilon states, and predictions of dominant decay of the Higgs boson into hadronic jets.

In addition to his presentation at the Amsterdam conference, Berger spoke during the second half of 2002 about this work also in seminars at Cambridge University, England; University of California, Riverside; CERN, Geneva, Switzerland; and Cornell University.

(E. L. Berger)

II.A.4. e^+e^- Annihilation into $J/\psi + J/\psi$ at *B* Factories

Recent measurements by the Belle Collaboration of the cross section for $e^+e^- \rightarrow J/\psi + \eta_c$ are about an order of magnitude larger than existing calculations. This is a challenge to our current understanding of charmonium production, which is based on Non-relativistic QCD (NRQCD).

States such as $J/\psi + \eta_c$, consisting of two charmonia in opposite charge-conjugation states, can be produced in an order$-\alpha^2\alpha_s^2$ process involving a virtual photon and a virtual gluon. On the other hand, states such as $J/\psi + J/\psi$, consisting of two charmonia in opposite charge-conjugation states, cannot be produced in an order$-\alpha^2\alpha_s^2$ process. Therefore, one might expect production of $J/\psi + J/\psi$ to be suppressed relative to production of $J/\psi + \eta_c$.

Both of the states $J/\psi + \eta_c$ and $J/\psi + J/\psi$ can be produced in a purely electromagnetic process of order α^4, which involves two virtual photons. One would expect such a process to be suppressed by $\alpha^2 \alpha_s^2$, relative to the photon-gluon process for $J/\psi + \eta_c$ production. However, G. Bodwin, E. Braaten (Ohio State), and J. Lee observed that the suppression factor for the electromagnetic process can be overcome by kinematic enhancements. Specifically, for states such as $J/\psi + J/\psi$, consisting of two charmonia in opposite charge-conjugation states, the production can proceed through the fragmentation of each photon into a J/ψ. The fragmentation process is kinematically enhanced because the photon propagators are of order $1/(2m_c)^2$, whereas photon and gluon propagators are of order $1/s$ in non-fragmentation processes. The $\bar{c}c$ electromagnetic currents yield numerator factors m_c, and, so, the net enhancement factor is $s^2/(2m_c)^4$. In addition, the angular distribution for the fragmentation process is sharply peaked along the beam directions. The peaking arises from would-be collinear divergences that are cut off by m_c. They yield an additional enhancement factor in the total rate of $\log[s^2/(2m_c)^4]$. The exact calculation shows that the rate for $e^+ e^- \to J/\psi + J/\psi$ is about 3.7 times the rate for $e^+ e^- \to J/\psi + \eta_c$. Perturbative-QCD and relativistic corrections have not been computed for all of the electromagnetic contributions, but they are estimated to be large. For the pure fragmentation contribution to $e^+ e^- \to J/\psi + J/\psi$, they reduce the rate by about a factor 3.

The Belle Collaboration measurement of the rate for production of $J/\psi + \eta_c$ identifies the η_c by reconstructing the mass of the decay products. However, the Belle mass resolution near the η_c mass is about 0.11 GeV, while the splitting between the J/ψ and the η_c is only 0.12 GeV. Bodwin, Braaten, and Lee suggested that the Belle $J/\psi + \eta_c$ signal may actually include $J/\psi + J/\psi$ events. If that is the case, then the discrepancy between experiment and theory could be reduced significantly.

This work is described in ANL-HEP-PR-02-110 [hep-ph/0212181] and ANL-HEP-PR-02-105 [hep-ph/0212352].

(G. T. Bodwin)

II.A.5. Lattice Gauge Theory

During this period we have continued our studies of hadronic matter in extreme environments using lattice gauge theory simulations. Because of the sign problems associated with systems at finite baryon-number density, we have limited our finite density studies to QCD at finite isospin density (and temperature) and 2-flavour QCD at finite quark-number density. For our finite temperature studies we have continued to use a modified action which allows us to work at zero quark mass.

Previously we had verified the expectation that 2-colour $(SU(2)_{colour})$ QCD undergoes a phase transition with mean-field critical exponents to a phase characterized by a di-quark condensate, which spontaneously breaks quark number. We have now completed our simulations of this theory at $4/g^2 = 1.5$ and small quark mass $m = 0.025$ on a $12^3 \times 24$ lattice. We are now commencing analyses of the Goldstone and pseudo-Goldstone spectra, using the scalar and pseudoscalar meson/diquark propagators these simulations generated, which will yield further understanding of this superfluid phase, and serve to further differentiate it from the normal phase.

We have been simulating lattice QCD with a finite chemical potential μ_I for isospin (I_3) and finite temperature T on $8^3 \times 4$ lattices. Here we are studying the μ_I dependence of the transition temperature T_c where hadronic matter converts to a quark-gluon plasma (Fig. 1). At low μ_I, this also yields the quark-number chemical potential dependence of T_c. (This includes the regime accessible to RHIC.) During this period we have been extending this range of μ_I to the boundary of the pion condensed phase. We have also commenced simulations on a $16^3 \times 4$ lattice at a relatively high $\mu = 0.8 > \mu_c \approx 0.56$ to confirm earlier indications that the transition, which is now characterized by the evaporation of the pion condensate, has become first order.

We are simulating lattice QCD with massless u and d quarks on $16^3 \times 8$ and $24^3 \times 8$ lattices using a lattice action enhanced by an irrelevant chiral 4-fermion interaction, which preserves the lattice symmetries. Here we expect to determine the universality class of the finite temperature phase transition from hadronic matter to a quark-gluon plasma. So far we have been able to determine the range of couplings which span the transition value.

Our simulations used the NERSC and NPACI IBM SP's, the IBM Regatta at Boston University, the HP Superdome at the University of Kentucky and the Linux PC on my desk.
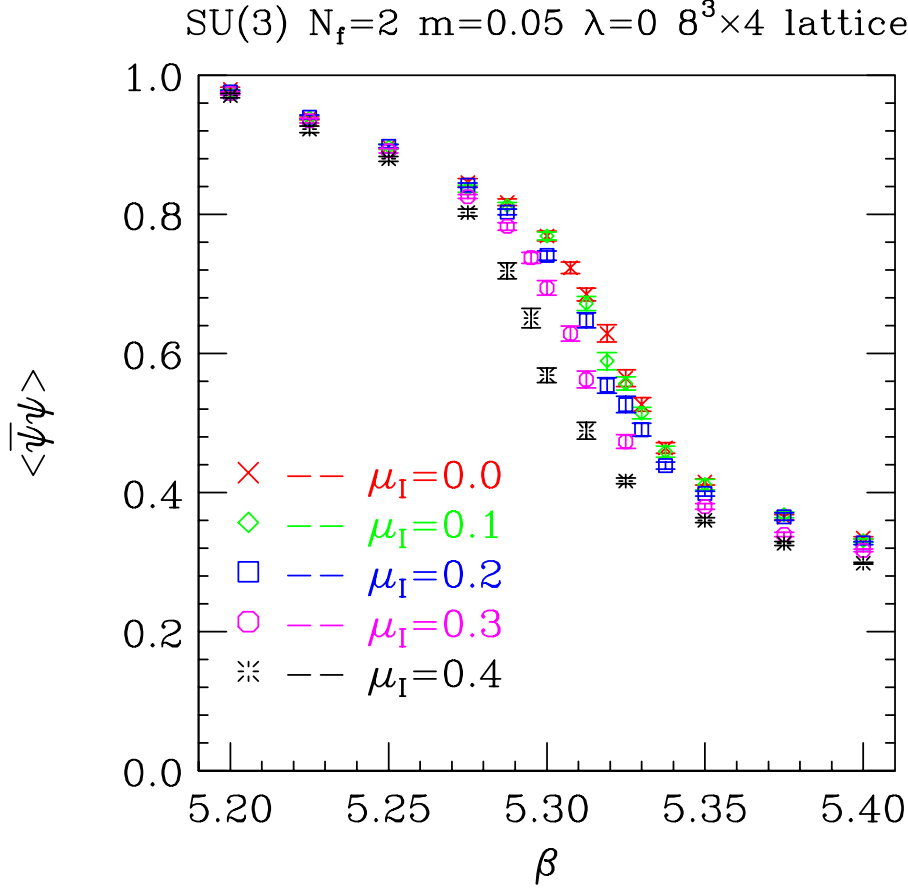
Figure 1. The chiral condensate as a function of $\beta = 6/g^2$ for a range of μ_I values. Note that the position of the transition moves to lower β and hence temperature as μ_I is increased.

(D. K. Sinclair)

II.A.6. Electroweak Baryogenesis and Supersymmetry

Electroweak baryogenesis provides a predictive framework for the computation of the baryon asymmetry of the universe. Perhaps the most attractive feature of this mechanism is that it relies on anomalous baryon number violation processes, which are present in the Standard Model. At temperatures far above the electroweak phase transition scale, these anomalous processes are unsuppressed and, in the absence of any $B - L$ asymmetry, lead to the erasure of any baryon or lepton number generated at high energy scales. These baryon number violation processes are, instead, exponentially suppressed in the electroweak symmetry broken phase, at temperatures far below the electroweak phase transition. The mechanism of electroweak baryogenesis may become effective if the CP-violating sources are strong and, at the electroweak

phase transition temperature, the baryon number violation processes in the broken phase are sufficiently suppressed, leading to a baryon number density in the broken phase consistent with observations. This, in turn, demands a strongly first order electroweak phase transition.

It has been long ago realized that in the Standard Model the CP violating sources are too weak to lead to an acceptable baryon number density. Moreover, even if the sources were strong enough to lead to a reasonable baryon number generation, for the Higgs masses consistent with the present experimental constraints the electroweak phase transition is a cross-over, implying that baryon number violating processes are in equilibrium at the electroweak phase transition and leading to no baryon number generation in the broken phase. A minimal supersymmetric extension of the Standard Model (MSSM), instead, has all the necessary ingredients to improve on both problems. First, there are additional sources of CP-violation associated with the CP-violating phases of the supersymmetry breaking parameters. Second, in the presence of a light stop, the phase transition may become strong enough to allow the preservation of the baryon number generated at the electroweak symmetry breaking scale.

In a very recent work [Nucl. Phys. **B650**, 24 (2003)], we have improved on previous computations of the baryon asymmetry, by deriving the diffusion equations and the sources for the generation of baryon number. Within the present framework, the CP-violating forces are provided by the interaction of the different fields with the Higgs profiles, which vary along the bubble wall. These CP-violating forces induce CP-violating currents for the different fields, which lead to non-zero densities $\left(n_i, j_i^z\right)$ after elastic and inelastic interactions, with the other fields present in the plasma.

$$-v_w n_i' + D_i n_i'' + \Gamma_{ij} \frac{n_j}{k_j} = S_i\left[n^{(B)}\right], \tag{1}$$

where the source is given by

$$S_i = D_i \left(n_i^{(B)}\right)'' - v_w \left(n_i^{(B)}\right)' \simeq D_i \left(n_i^{(B)}\right)'', \tag{2}$$

where D_i is the diffusion constant, v_ω is the velocity of the wall of the expanding true-vacuum bubble, Γ_{ij} represents the rate of a given process involving interaction of the particle i with the particle j, k_j is a statistical factor, $k_j = 2$ ($k_j = 1$) for bosons (fermions), and $n_i^{(B)}$ is the current density in the Higgs background provided by the expanding bubble. The detailed evaluation of the currents necessary to compute the sources for the diffusion equations was provided in a previous article [Nucl. Phys. **B599**, 158 (2001)].

The left-handed quark chemical potentials receive two contributions. The dominant one may be obtained by solving the diffusion equation for the different colors of quarks in the

presence of gauge, Yukawa, mass and strong sphaleron interactions. Because no baryon number violating processes are included, the solutions to these diffusion equations lead to an equal number of baryons of a given chirality and antibaryons of the opposite chirality. These dominant densities may be considered as approximately constant during the characteristic long times in which the weak sphaleron processes take place.

The left-handed densities receive also a subdominant contribution coming from the weak sphaleron interactions. This contribution is associated with a net-baryon number, which, considering effective mixing between the different flavors and colors of quarks, is shared in approximately equal parts by all 36 of them. One arrives to the equation

$$Dn_B''(z) - v_w n_B'(z) = \theta(-z)_{ws}\left(\frac{3T^2 \mu_L^{diff}(z)}{4} + An_B(z)\right),$$ (3)

where n_B is the baryon number density, $\Gamma_{ws} = 6k_{ws}\alpha_w^5 T$ (α_w is the weak coupling constant), with $k_{ws} \simeq 20$ being the weak sphaleron rate, while μ_L^{diff} is equal to the sum over the three generations of the left-handed up and down quark chemical potentials associated with a given color of quarks, as obtained by solving their diffusion equations in the absence of the slow sphaleron interactions. In the numerical simulations, we have considered heavy all squarks and sleptons except for the lightest stop, in which case the coefficient $A = 24/7$, which differs only slightly from the SM result $A^{SM} = 15/4$.

In Fig. 1, we show the comparison of the baryon number to entropy ratio η computed within the present model with the mean value of the one consistent with Big Bang Nucleosynthesis (BBN). The results are plotted as a function of the Higgsino mass parameter μ, for values of the weak gaugino masses $M_2 = |\mu|$, and for different values of the CP-odd Higgs mass m_A. We have chosen soft supersymmetry breaking parameters in the stop sector such that they lead to a value of the Higgs boson mass consistent with the present experimental constraints, and the lightest stop light enough so that the phase transition becomes strongly first order, $v(T)/T \gtrsim 1$.

51

$M_2 = \mu$
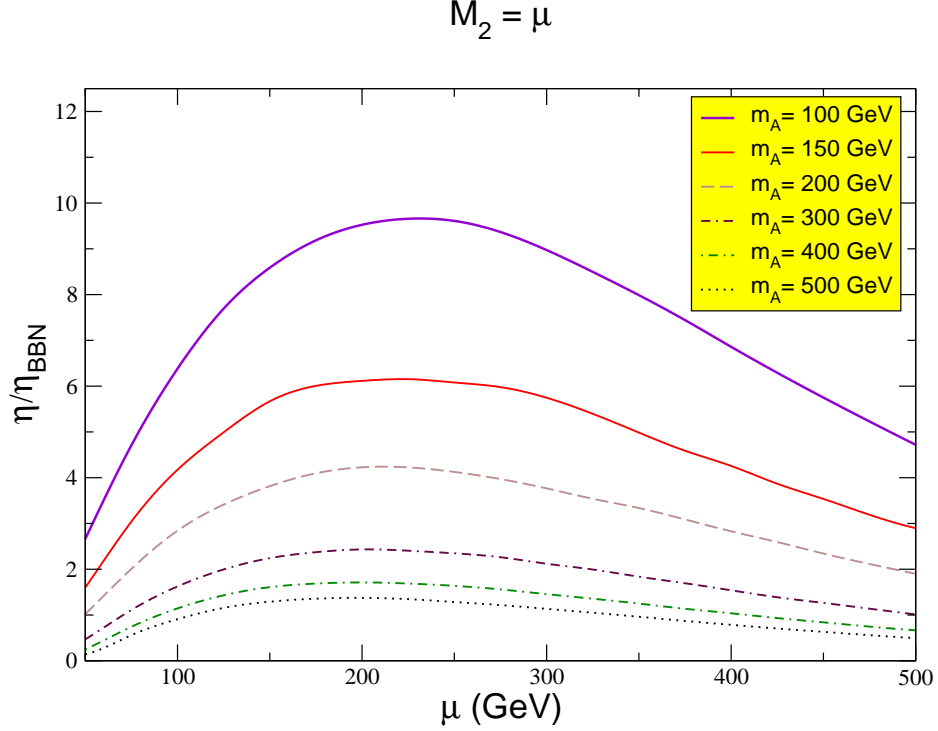
Figure 1. Plot of η/η_{BBN} as a function of μ for $\tan\beta = 10$, $M_2 = \mu$ and the specified values of m_A.

We have chosen a maximal value of the phase of the μ parameter, $\sin\phi_\mu = 1$. Therefore, the inverse of the values shown in the figure can be interpreted as the value of $\sin\phi_\mu$ necessary to obtain a prediction consistent with BBN. Our calculations lead to a bound on the value of the CP-violating phase, $\sin\phi_\mu \gtrsim 0.1$, but due to the natural uncertainties associated with our simplified treatment of the baryon asymmetry calculation, and the experimental error in the determination of η_{BBN}, we cannot reliably rule out the possibility that somewhat smaller values of the phase ϕ_μ may lead to consistency with the BBN predictions.

(C.E.M. Wagner)

II.A.7. Consistent Quantization of Nambu Brackets

The classical evolution of topological N-branes is specified by Nambu Brackets (NB), but quantization of such membranes has been held up by perceived inconsistencies in quantizing these brackets, a nagging problem since their inception in 1973. C. Zachos and T. Curtright (U Miami) applied results of theirs on the deformation quantization of superintegrable systems, [hep-th/0210170, ANL-HEP-CP-02-089; and math-ph/0211021, ANL-HEP-CP-02-102] to explicitly test NB quantization proposals, through direct comparison to the conventional

quantum answers thus found. The first of these papers establishes compatibility of the results with the Groenewold-van Hove theorem--indeed, necessity, and the second quantizes further superintegrable systems in phase-space.

Maximally superintegrable systems, classically, have their invariants entering into NBs, to yield an alternate specification of their dynamics. Zachos and Curtright thus showed how Nambu's early quantization prescription can, indeed, succeed, despite widespread expectations to the contrary: comparison to the deformation quantization results found in this project vindicates Nambu's prescription (and invalidates other prescriptions), for systems in a large class. More generally, it argues against unrealistic desiderata broadly held, such as reliance on classical identities improperly generalized to the quantum domain. The quantization method thus developed is detailed in a 44p paper [hep-th/0212267, ANL-HEP-PR-02-109], now formulated entirely through operators in Hilbert space--not phase space. It resolves most consistency conundrums on the quantization of NBs, exhausts the discussion of the correct identities to be considered, illustrates the method through half a dozen explicit applications, and re-frames the issues properly in a way conducive to progress in M-theory. It should serve as the sourcebook for further application in membrane quantization efforts in the HEP community.

(C. Zachos)

III.   ACCELERATOR RESEARCH AND DEVELOPMENT

III.A.   ARGONNE WAKEFIELD ACCELERATOR PROGRAM

III.A.1. The Argonne Wakefield Accelerator Status

During this period, we continued the new AWA RF photocathode gun and laser upgrades. The electron beam with charge of a few nC was produced using the new laser beam. We have amplified the laser beam from the Ti:Sapphire laser in the existing Lambda LPX105i excimer laser. We achieved energy output of 15 mJ from the excimer laser. With a new magnesium cathode implemented and amount of the laser energy available, we expect to obtain more than 100 nC electron beam from the new gun. We have investigated the beam diagnostics such as optical transition radiation for bunch length measurement. A large metal mirror and an emittance plate were installed in diagnostic ports and ready for the experiment.

A process of replacing the existing AWA Control is completed. A new PC based control computer and two PC controllers for CAMAC were installed. We developed a new NT based control programs using National Instrument's LabWindow/CVI system. All system software and hardware were tested and switched over.

III. A. 2. The New Type of Dielectric Accelerator Development

Due to the coupling problems developed during the high power tests for dielectric structures at NRL, we have re-examined the coupling schemes. We have found a new modular type coupling structures as shown in Figure 1. The scheme as a few advantages: The modular approach has several advantage: separate Coupling Problem from Acceleration; the coupling does not depend on location of taper with respect to the aperture; copper residue on outside of dielectric won't be harmful; larger coupling- aperture lowers the power density. We have fabricated and cold tested an Alumina based structure and the results are in good agreement with the theory and simulation. High power test will proceed in a few months when NRL facility became available.
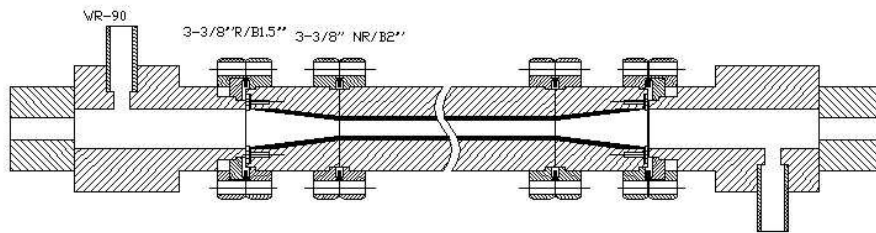
Figure 1. Design of a modular traveling wave dielectric structures.
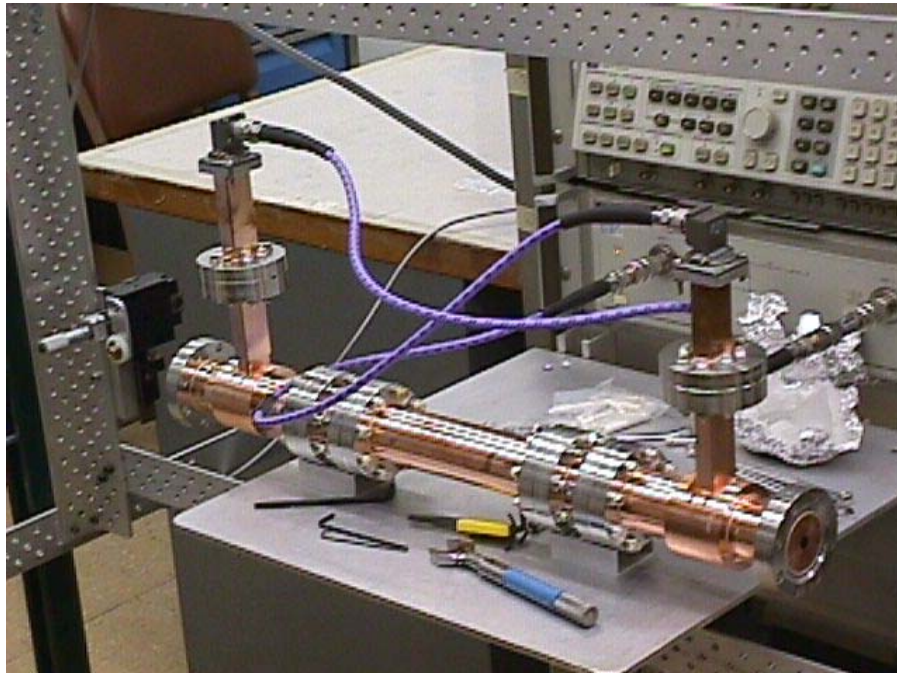
Figure 2. A newly fabricated dielectric accelerator under the bead pull test.
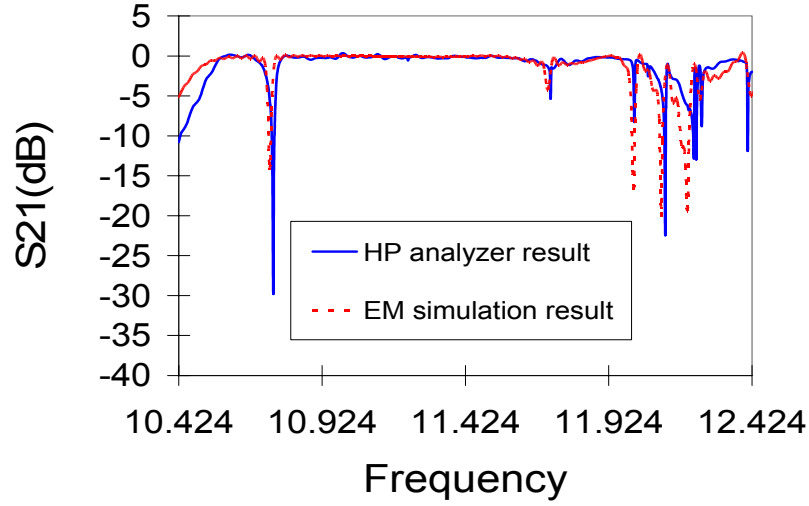
Figure 3. Measured RF transmission through the newly designed coupler and its comparison with the simulations.

III. A. 3. High power 21 GHz RF generation using Dielectric Tubes at CERN

In collaboration with SLAC, we developed a dielectric based decelerator as a power extraction device for CLIC. Working with DULY research, we have designed and fabricated a dielectric based power extraction device. An experiment was performed at the CLIC test facility, and produced up to 20 ~ 50 MW RF power at 21 GHz. This is equivalent of 20 – 40 MV/m axial electric field produced. However, the output coupler network was not optimized, resulting in significant reflection losses. A new round of high power testing will be conducted at our AWA facility with a pulse train generated from the AWA gun. Figure 4 shows the experimental data obtained during the run and it shows the measured trapped RF power in the tube.
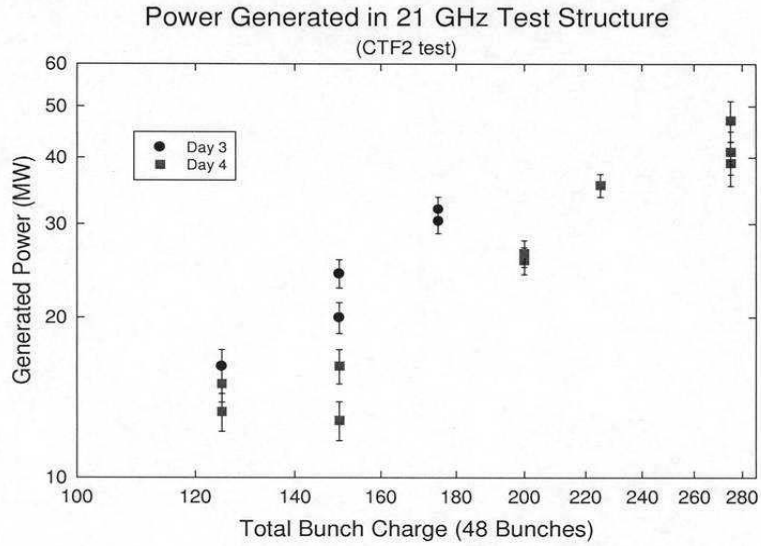
Figure 4. Power generated in the 21 GHz dielectric power extractor at CERN

(W. Gai)

III. B.   MUON COLLABORATION R & D

a)   Muon Ionization Cooling Experiment

The primary effort during this period was devoted to measuring electrons and x-rays produced by field emission from the 805 MHz pillbox cavity in Lab G. This data was then used to construct an argument that the backgrounds in the proposed Muon Ionization Cooling Experiment (MICE) would be at a level that was acceptable for the proposed silicon fiber and Gaseous Electron Multiplier (GEM) detectors. The measurements included dark current and x-ray measurement, both intensity and spectra, with and without an axial solenoidal field of 2.5 T. This data was then written up by Norem of ANL and McKigney, of Imperial College London, into Chapter 9 of the MICE experimental proposal. Final editing of the proposal was done by A. Blondel of the University of Geneva. The proposal, representing the work of 140 people from 35 institutions, was submitted to Rutherford Appleton Lab at the beginning of the year.

There were a few surprises in the data from Lab G. The primary one was that when the solenoidal magnetic field was turned on, the cavity became much more sensitive to breakdown and sparking. This damage was initially not affected by conditioning procedures which have in the past helped the cavity recover its operating electric field at a given magnetic intensity. However continued operation, (almost 4 weeks), with the magnetic field off produced better electric field values.

We began a series of measurements with a 2.T solenoidal field in a cavity that routinely operated at 34 MV/m with very low dark currents. A pillbox cavity, where the electric field is always perpendicular to the end windows, may be particularly susceptible to magnetic field effects. Magnetic fields pin dark current beams to magnetic field lines so the low field AC components cannot spray the beams over a larger area. In addition, since the electric and magnetic fields are parallel, there are no E x B drifts to increase the beam emittance and the energy density is further enhanced. Dark current beams thus traverse the cavity and arrive at the opposite wall with very high energy density, which could damage the wall or produce other emitters. Our data seem to confirm this model, since operation with a solenoidal field produced more sparking and significantly larger field enhancements, and these enhancements persisted even after the magnetic field was turned off.

During this time we also measured the x-ray spectrum produced in the cavity using an ORTEK germanium detector. The spectra measured seem to show an E^{-3} dependence, which is much steeper than what would be expected from low energy bremsstrahlung. We assume that what is happening is that the low energy spectra incorporate considerable absorption and scattering.

b)   Understanding and Extending the Limits of RF Cavities

Although the future of High Energy Physics seems to depend fairly directly on the limits of electric field gradients in rf cavities, there is little effort directed specifically at the relevant material science aspects of this problem. During this period we submitted a proposal for Laboratory support and were funded for some initial work on understanding and extending the limits of rf cavities. This effort will involve both experimental and theoretical work to determine and model the significant effects involved in limiting rf cavity gradients, in addition to testing materials and techniques which can improve their performance.

We have started both experimental and theoretical work and Ahmed Hassanein and Isak Konkashbaev of ET are collaborating on this effort. Experimental work started with a measurement of the Preston coefficient for fluid polishing with cerium oxide to determine if this method could be used to produce large smooth copper surfaces.   This number relates the mass removal rate with the pressure, velocity and tangential force exerted by a polishing element. The results showed that the material removal rates were probably too low for this method to be useful.   Theoretical effort started with an initial survey of mechanisms involved with rf interactions with cavity walls. Although these phenomena have been discussed for many years, the quality of experimental data is low, and theoretical models seem to systematically omit significant processes. Thus it seems necessary to begin fairly independently of existing work, after, of course, becoming familiar with it.

(J. Norem)

IV. PUBLICATIONS

IV. A. Books, Journals And Conference Proceedings

A Gigabit Ethernet Link Source Card
>R. E. Blair, J. W. Dawson, G. Drake, W. N. Haberichter, J. L. Schereth
>>In: *Proceedings of the 8th Workshop on Electronics for the LHC Experiments 278-280*
>>Colmar, France (September 9-13, 2002).

Azimuthal Anisotropy of K_s° and Λ and $\overline{\Lambda}$ Production at Mid-Rapidity from Au+Au Collisions at $\sqrt{S_{NN}}$ = 130 GeV
>R. V. Cadman, K. Krueger, H. M. Spinka, D. G. Underwood
>>Phys. Rev. Lett. **89**, 132301 (September 2002).

$B \rightarrow D_s \pi$ and the Tree Amplitude in $B \rightarrow \pi^+ \pi^-$
>C.-W. Chiang, Z. Luo, and J. L. Rosner
>>Phys. Rev. **D66**, 057503 (September, 2002).

Branching Ratio Measurements of Exclusive B^+ Decays to Charmonium with the Collider Detector at Fermilab
>R. E. Blair, K. L. Byrum, E. Kovacs, S. E. Kuhlmann, T. LeCompte, L. Nodulman, J. Proudfoot, R. Thurman-Keup, R. G. Wagner, A. B. Wicklund
>>Phys. Rev. **D66**, 052005 (September, 2002).

Branes and Orbifolds are Opaque
>M. Carena, T.M.P. Tait, and C.E.M. Wagner
>>Acta Physica Polonica **B33**, 2355-84 (September 2002).

Centrality Dependence of High p_t Hadron Suppression in Au+Au Collisions at $\sqrt{S_{NN}}$ = 130 GeV
>R. V. Cadman, K. Krueger, H. M. Spinka, D. G. Underwood
>>Phys. Rev. Lett. **89**, 202301 (November 2002).

Chiral Anomaly and High-Energy Scattering in QCD
>A. R. White
>>Phys. Rev. **D66**, 056007 (September 2002).

Chirality Violation in QCD Reggeon Interactions
>A.R. White
>>Phys. Rev. **D66**, 045009 (August 2002).

Cross Section for Forward J/ψ Production in $p\bar{p}$ Collisions at $\sqrt{s} = 1.8$ TeV
> R. E. Blair, K. L. Byrum, E. Kovacs, S. E. Kuhlmann, T. LeCompte, L. Nodulman, J. Proudfoot, R. Thurman-Keup, R. G. Wagner, A. B. Wicklund
>> Phys. Rev. **D66**, 092001 (November 2002).

Coherent $p°$ Production in Ultra-Peripheral Heavy Ion Collisions
> R. V. Cadman, K. Krueger, H. M. Spinka, D. G. Underwood
>> Phys. Rev. Lett. **89**, 272302 (December 2002).

Cosmological Constant in Broken Maximal Sugras
> G. Chalmers
>> Class. Quant. Grav. **19**, L193-L198 (November 2002).

Deformation Quantization of Superintegrable Systems and Nambu Mechanics
> T. L. Curtright and C. K. Zachos
>> New J. Phys. **4**, 83 (October 2002).

Elastic Scattering and Direct Detection of Kaluza-Klein Dark Matter
> G. Servant and T.M.P. Tait
>> New J. Phys. **4**, 99 (December 2002).

Elliptic Flow from Two- and Four-Particle Correlations in Au + Au Collisions at $\sqrt{S_{NN}} = 130$ GeV
> R. V. Cadman, K. Krueger, H. M. Spinka, D. G. Underwood
>> Phys. Rev. **C66**, 034904 (September 2002).

Experimental Challenges for QCD—The Past and the Future
> H. Lipkin
>> In: *Proceedings of the Symposium and Workshop, "Continuous Advances in QCD 2002/Arkadyfest"* ed. by K. A. Olive, et al. (World Scientific, Singapore, 2002) pp. 153-166.

Higgs Boson Decay into Hadronic Jets
> E. L. Berger, C.-W. Chiang, J. Jiang, T.M.P. Tait, and C.E.M. Wagner
>> Phys. Rev. **D66**, 095001 (November 2002).

High Power Testing of ANL X-Band Dielectric-Loaded Accelerating Structures
> John Power, Wei Gai, Chunguang Jing, Richard Konecny, Steven H. Gold and Allen K. Kinkead
>> In: *Conference Proceedings to Advanced Accelerator Concepts* June 22-28, 2002, Oxnard, CA, Vol. **647**, 556-564 June, 2002. (*not previously cited*)

Lattice QCD at Finite Isospin Density at Zero and Finite Temperature
    B. Kogut and D. K. Sinclair
        Phys. Rev. **D66**, 034505 (2002).

Limits on Extra Dimensions and New Particle Production in the Exclusive Photon and Missing Energy Signature in $p\overline{p}$ Collisions at $\sqrt{s}$ = 1.8 TeV
    R. E. Blair, K. L. Byrum, E. Kovacs, S. E. Kuhlmann, T. LeCompte, L. Nodulman,J. Proudfoot, R. Thurman-Keup, R. G. Wagner, A. B. Wicklund
        Phys. Rev. Lett. **89**, 281801 (December, 2002).

Measurement of Analyzing Power for Proton-Carbon Elastic Scattering in the Coulomb-Nuclear Interference Region with a 22-GeV/c Polarized Proton Beam
    D. Underwood
        Phys. Rev. Lett. **89**, 052302 (July 2002).

Measurement of Diffractive Production of D*$^{\pm}$(2010) Mesons in Deep Inelastic Scattering at HERA
    S. Chekanov, D. Krakauer, S. Magill, B. Musgrave, J. Repond, R. Yoshida
        Phys. Lett. **B545**, 244-260 (2002).

Measurements of Inelastic J/ψ and ψ' with Photoproduction at HERA
    S. Chekanov, D. Krakauer, S. Magill, B. Musgrave, J. Repond, R. Yoshida
        Eur. J. Phys. **C27**, 173-188 (2002).

Measurement of the Q$^{\wedge}$2 and Energy Dependence of Diffractive Interactions at HERA
    S. Chekanov, D. Krakauer, S. Magill, B. Musgrave, A. Pellegrino, J. Repond, R. Yoshida
        Eur. J. Phys., **C25**, 169-187 (2002).

Measurement of the Ratio of B Quark Production Cross Sections in $p\overline{p}$ Collisions at $\sqrt{s}$ = 630 GeV and $\sqrt{s}$ = 1800 GeV
    R. E. Blair, K. L. Byrum, E. Kovacs, S. E. Kuhlmann, T. LeCompte,
    L. Nodulman, J. Proudfoot, R. Thurman-Keup, R. G. Wagner, A. B. Wicklund
        Phys. Rev. **D66**, 032002, (2002).

Mid-Rapidity Λ and $\overline{\Lambda}$ Production in Au + Au Collisions at $\sqrt{S_{NN}}$ = 130 GeV
    H. M. Spinka, D. G. Underwood, R. V. Cadman, K. Krueger
        Phys. Rev. Lett. **89**, 092301 (August 2002).
Mid-Rapidity ϕ Production in Au+Au Collisions at $\sqrt{S_{NN}}$ = 130 GeV
    R.V. Cadman, K. Krueger, T. LeCompte, H.M. Spinka, D.G. Underwood
        Phys. Rev. **C65**, 041901 (R) 2002.

Multi-Hadron Final States
    J. Repond
        In: *Proceedings of the X International Workshop on Deep Inelastic Scattering (DIS2002),* Krakow, Poland (April 30-May 4, 2002).
        Acta Phys. Polon, **B33**, 3329 (2002).

Order-v^4 Corrections to S-wave Quarkonium Decay
    G. T. Bodwin and A. Petrelli
        Phys. Rev. **D66**, 094011 (November 2002).

Polarization of Prompt J/ψ and Y(*nS*)
    J. Lee
        In: *Proceedings of the X International Workshop on Deep Inelastic Scattering* (DIS2002).Acta Physica Polonica **B33**, 3237-3241 (October 2002).

Quenched Lattice QCD at Finite Isospin Density and Related Theories
    J. B. Kogut and D. K. Sinclair
        Phys. Rev. **D66**, 014508 (July, 2002).

Search for New Physics in Photon-Lepton Events in $p\bar{p}$ Collisions at $\sqrt{s}$ = 1.8 TeV
    R. E. Blair, K. L. Byrum, E. Kovacs, S. E. Kuhlmann, T. LeCompte, _L. Nodulman, J. Proudfoot, R. Thurman-Keup, R. G. Wagner, A. B. Wicklund
        Phys. Rev. Lett. **89**, 041802, (July, 2002).

Search for Neutron-Antineutron Oscillations Using Multiprong Events in Soudan 2
    D. S. Ayres, T. H. Fields, M. C. Goodman, T. Joffe-Manor, J. Thron
        Phy. Rev. **D66**, 032004 (2002).

Search for Radiative b-Hadron Decays in $p\bar{p}$ Collisions at $\sqrt{s}$ = 1.8 TeV
    R. E. Blair, K. L. Byrum, E. Kovacs, S. E. Kuhlmann, T. LeCompte, L. Nodulman, J. Proudfoot, R. Thurman-Keup, R. G. Wagner, A. B. Wicklund
        Phys. Rev. **D66**, 11202 (December 2002).

Suggestions for Benchmark Scenarios for MSSM Higgs Boson Searches at Hadron Colliders
    M. Carena, S. Heinemeyer, C.E.M. Wagner, and G. Weiglein
        A brief version appears In: *Proceedings of the Workshop on Physics at TeV Colliders* (Les Houches 2001), ed. by P. Aurenche, *et al*. (Paris, October 2002) pp. 22-24.

Summary: Working Group on QCD and Strong Interactions
> E. L. Berger, …S. Magill, *et al.*
>> In: *Proceedings of the APS/DPF/DPB Summer Study on the Future of Particle Physics* (Snowmass 2001),
>> eConf C010630, **P5001** (June 2002).

The Chiral Anomaly and High-Energy Scattering in QCD
> A. R. White
>> Phys. Rev. **D66**, 056007 (September 2002).

The Higgs Working Group: Summary Report (2001)
> D. Cavalli, …. C.E.M. Wagner, et al.
>> In: *Proceedings of the Workshop on Physics at TeV Colliders* ed. by P. Aurenche, et al (Paris, October 2002) pp. 1-120.

The Phase Diagram of Four Flavor SU(2) Lattice Gauge Theory at Nonzero Chemical Potential and Temperature
> J. B. Kogut, D. Toublan, and D. K. Sinclair
>> Nucl. Phys. **B642**, 181-209 (October, 2002).

The Snowmass Points and Slopes: Benchmarks for SUSY Searches
> B. C. Allanach, ...C.E.M. Wagner, et al.
>> Eur. Phys. J. **C25**, 113-123 (July 2002).

Top-Squark Searches at the Tevatron in Models of Low-Energy Supersymmetry Breaking
> M. Carena, D. Choudhury, R. A. Diaz, H. E. Logan and C.E.M. Wagner
>> Phys. Rev. **D66**, 115010 (December 2002).

Uncertainties on the Measurements of the Top Mass at a Future e^+e^- Collider
> S. Chekanov
>> Eur. J. Phys., **C26**, 173-181 (2002).

Wakefield Acceleration in Structures
> Manoel E. Conde
>> In: *Conference Proceedings to Advanced Accelerator Concepts 2002*, Oxnard, CA, June 22-28, 2002.
>> Vol. **647**, 63-70 (2002).

IV.B. Major Articles Submitted For Publication

805 MHz and 201 MHz RF Cavity Development for MUCOOL
J. Norem
Journal of Phys. G
ANL-HEP-PR-02-121

Branes and Orbifolds are Opaque
M. Carena, T.M.P. Tait, and C.E.M. Wagner
Acta Physica Polonica B
ANL-HEP-PR-02-043

Classical and Quantum Nambu Mechanics
T. Curtright and C. Zachos
Phys. Rev. D.
ANL-HEP-PR-02-109

Collider Probes of the MSSM Higgs Sector with Explicit CP Violation
M. Carena, J. Ellis, S. Mrenna, A. Pilaftsis, and C.E.M. Wagner
Phys. Phys. D
ANL-HEP-PR-02-104

Current LH_2 Absorber R&D in MuCool
J. Norem
Journal of Phys. G
ANL-HEP-PR-02-122

Determining tan β with Neutral and Charged Higgs Bosons at a Future e^+e^- Linear Collider
J. Gunion, T. Han, J. Jiang, and A. Sopczak
Phys. Lett. B
ANL-HEP-PR-02-090

Differential Cross Section for Higgs Boson Production Including All-Orders Soft Gluon Resummation
E. L. Berger and J.-W. Qiu
Phys. Rev. D
ANL-HEP-PR-02-057

Disappearance of Back-to-Back High pT Hadron Correlations in Central Au+Au Collisions at $\sqrt{S_{NN}} = 200$ GeV
R. V. Cadman, K. Krueger, H. M. Spinka, D. G. Underwood
Phy. Rev. Lett.
ANL-HEP-PR-02-112

e^+e^- Annihilation into $J/\psi + J/\psi$
> G. T. Bodwin, J. Lee, and E. Braaten
>> Phys. Rev. Letts.
>> ANL-HEP-PR-02-110

Elastic Scattering and Direct Detection of Kaluza-Klein Dark Matter
> G. Servant and T.M.P. Tait
>> New J. Phys.
>> ANL-HEP-PR-02-054

Exclusive Double-Charmonium Production from e^+e^- Annihilation into a Virtual Photon
> E. Braaten and J. Lee
>> Phys. Rev. D
>> ANL-HEP-PR-02-094

Exclusive Double-Charmonium Production from e^+e^- Annihilation into Two Virtual Photons
> G. T. Bodwin, J. Lee, and E. Braaten
>> Phys. Rev. D
>> ANL-HEP-PR-02-105

Final State Phases in $B \to D\pi,\ D^*\pi,\ \text{and}\ D\rho$ Decays
> C.-W. Chiang and J. L. Rosner
>> Phys. Rev. D
>> ANL-HEP-PR-02-113

Improved Results in Supersymmetric Electroweak Baryogenesis
> M. Carena, M. Quiros, M. Seco, and C.E.M. Wagner
>> Nucl. Phys.
>> ANL-HEP-PR-02-041

Indirect Detection of Kaluza-Klein Dark Matter
> G. Bertone, G. Servant, G. Sigl
>> Phys. Rev. D
>> ANL-HEP-PR-02-099

Leading Proton Production in e^+p Collisions at HERA
> S. Chekanov, D. Krakauer, J. H. Loizides, S. Magill, B. Musgrave, J. Repond, R. Yoshida
>> Nucl. Phys. B
>> ANL-HEP-PR-02-096

Light Gluino and the Running of α_s
>C.-W. Chiang, Z. Luo, and J. L. Rosner
>>Phys. Rev. D
>>ANL-HEP-PR-02-055

Low Energy 6-Dimensional N=2 Supersymmetric SU(6) Model on T^2 Orbifolds,
>J. Jiang, T.-J. Li and W. Liao
>>Phys. Rev. D
>>ANL-HEP-PR-02-092

Measurement of High-Q^2 e⁻p Neutral Current Cross Sections at HERA and the Extraction of xF$_3$
>S. Chekanov, D. Krakauer, S. Magill, B. Musgrave, J. Repond, R. Yoshida
>>Eur. J. Phys.,
>>ANL-HEP-PR-02-080

Measurement of Proton-Dissociative Diffractive Photoproduction of Vector Mesons at Large Momentum Transfer at HERA
>S. Chekanov, D. Krakauer, S. Magill, B. Musgrave, J. Repond, R. Yoshida
>>Eur. J. Phys.

Momentum Distribution of Charged Particles in Jets in Dijet Events in $\rho\bar{\rho}$ Collisions at $\sqrt{s_{NN}} =$ 1.8 TeV and Comparisons to Perturbative QCD Predictions
>R. E. Blair, K. L. Byrum, E. Kovacs, S. E. Kuhlmann, T. LeCompte, L. Nodulman, J. Proudfoot, R. Thurman-Keup, R. G. Wagner, A. B. Wicklund
>>Phys. Rev. D
>>ANL-HEP-PR-02-051

Observation of the Strange Sea in the Proton via Inclusive phi-Meson Production in Neutral Current Deep Inelastic Scattering at HERA
>S.Chekanov, D. Krakauer, S. Magill, B. Musgrave, J. Repond, R. Yoshida
>>Phys. Lett.
>>ANL-HEP-PR-02-106

Opaque Branes in Warped Backgrounds
>M. Carena, E. Ponton, T.M.P. Tait and C.E.M. Wagner
>>Phys. Rev. D
>>ANL-HEP-PR-02-115

Overcoming an Intrinsic Depolarizing Resonance with a Partial Snake at the Brookhaven AGS
>R. V. Cadman, H. Spinka, D. Underwood
>>Phys. Rev. ST Accel. Beams,
>>ANL-HEP-PR-02-068

Puzzles in Cabibbo-Suppressed Charm Decays
  F. E. Close and H. J. Lipkin
      Phys. Letts.
      ANL-HEP-PR-02-070

Search for W' Boson Decaying to a Top and Bottom Quarkin 1.8 TeV $p\bar{p}$ Collisions
  R. E. Blair, K. L. Byrum, E. Kovacs, S. E. Kuhlmann, T. LeCompte,
  L. Nodulman, J. Proudfoot, R. Thurman-Keup, R. G. Wagner, A. B. Wicklund
      Phys. Rev. Letts.
      ANL-HEP-PR-02-087

Strange Anti-Particle to Particle Ratios at Mid-Rapidity in $\sqrt{S_{NN}} = 130$ GeV Au+Au Collisions
  R. V. Cadman, K. Krueger, H. M. Spinka, D. G. Underwood
      Phys. Lett.
      ANL-HEP-PR-02-111

The $N_T = 4$ Finite Temperature Phase Transition for Lattice QCD with a Weak Chiral 4-Fermion Interaction
  J. B. Kogut and D. K. Sinclair
      Phys. Rev. D
      ANL-HEP-PR-02-091

Two-Body Cabibbo-Suppressed Charmed Meson Decays
  C.-W. Chiang, Z. Luo, and J. L. Rosner
      Phys. Rev. D
      ANL-HEP-PR-02-073

IV.C   Papers Or Abstracts Submitted To Conference Proceedings

Deformation Quantization, Superintegrability, and Nambu Mechanics
  C. K. Zachos and T. L. Curtright
      In: *Acta Physica Hungarica, Heavy Ion Physics 15, (2003).*
      ANL-HEP-CP-02-089

Design of Dielectric Accelerator Using TE-TM Mode Converter
  W. Liu, W. Gai
      In: *Advanced Accelerator Concepts 2002*, Oxnard, CA, June 22-28, 2002.
      ANL-HEP-CP-02-069

Description of EM Fields & Wakefields in Dielectric-Loaded Rectangular Waveguide Accelerating Structures
  L. Xiao, W. Gai, C. Jing and T. Wong
      In: *Advanced Accelerator Concepts 2002*, Oxnard, CA, June 22-28, 2002.
      ANL-HEP-CP-02-065

Jet Algorithms: A Mini-Review
  S. Chekanov
    In: *14th Topical Conference on Hadron Collider Physics*, Karlsruhe, Germany
    ANL-HEP-CP-02-103

Lattice QCD at Finite Isospin Chemical Potential and Temperature
  J. B. Kogut and D. K. Sinclair
    In: *Proceedings of the 20th International Symposium on Lattice Field Theory*
    (LATTICE 2002), Boston, MA, June 24-29, 2002.
    ANL-HEP-CP-02-062

Light Bottom Squark Phenomenology
  E. L. Berger
    In: *Proceedings of the 31st International Conference on High Energy Physics*
    (ICHEP 2002), Amsterdam, July 24-31, 2002.
    ANL-HEP-CP-02-085

Nambu Dynamics, Deformation Quantization, and Superintegrability
  T. L. Curtright and C. K. Zachos
    In: *Proceedings of the Workshop on Superintegrability in Classical and Quantum*
    Systems, Montreal, Canada*, September 16-21, 2002.
    ANL-HEP-CP-02-102

Other Atmospheric Neutrino Experiments
  M. Goodman
    In: *Proceedings of the XXth International Conference on Neutrino Physics and*
    Astrophysics, May 2002, Munich Germany.
    ANL-HEP-CP-02-075

Overview of tan β Determination at a Linear e^+e^- Collider
  J. Gunion, T. Han, J. Jiang, and A. Sopczak
    In: *Proceedings of the 10th International Conference on Supersymmetry and*
    Unification of Fundamental Interactions (SUSY02), Hamburg, Germany, 17-23
    June 2002.
    ANL-HEP-CP-02-118

Proton Beam Polarimetry at BNL
  Harold Spinka
    In: *Proceedings of the 15th International Spin Physics Symposium* (SPIN 2002).
    ANL-HEP-CP-02-093

QCD Physics in Atlas at the Large Hadron Collider
    J. Proudfoot
        In: *Proceedings of the 31st International Conference on High Energy Physics (ICHEP 2002)*, Amsterdam, July 24-31, 2002.
        ANL-HEP-CP-02-083

Recent Results on Quarkonium Production and Decay
    G. T. Bodwin
        In: *To appear in the Proceedings of the Conference on Quark Confinement and the Hadron Spectrum*, Gargnano, (Brescia), Italy, September 10-14, 2002.
        ANL-HEP-CP-02-114

RF Induced Backgrounds in MICE
    J. Norem, D. Li, A. Bross, A. Moretti, Y. Torun, E. McKignery
        In: *Proceedings of the NUFACT02* Conference, The Journal of Physics G.
        ANL-HEP-CP-02-088

Response to the Award of the Wigner Medal
    H. J. Lipkin
        In: *Proceedings of the 24th International Colloquium on Group Theoretical Methods in Physics*, Paris, July 14-20, 2002.
        ANL-HEP-CP-02-124

Results from the Argonne Wakefield Accelerator Test Facility
    W. Gai, M. Conde, R. Konecny, W. Liu, J. Power
        In: *Proceedings in Linac 2002, Pohang Accelerator Laboratory*, Gyeong Ju, Korea, Aug. 19-23, 2002.
        ANL-HEP-CP-02-108

SU(2) Lattice Gauge Theory at Nonzero Chemical Potential and Temperature
    J. B. Kogut, D. Toublan, and D. K. Sinclair
        In: *Proceedings of the 20th International Symposium on Lattice Field Theory* (LATTICE 2002), Boston, MA, 24-29 June 2002.
        ANL-HEP-CP-02-084

The Application of Lie Algebras to the Separation of Degrees of Freedom in Problems with Many Degrees of Freedom
    H. J. Lipkin
        In: *Proceedings of the 24th International Colloquium on Group Theoretical Methods in Physics*, Paris, July 14-20, 2002.
        ANL-HEP-CP-02-125

IV D.   Technical Reports And Notes

Technical Reports

Analysis of EB Support Saddles and Forces Between Modules During Assembly
     V. Guarino
          ANL-HEP-TR-02-058

Analysis of the Connections Between Modules in the EB
     V. Guarino
          ANL-HEP-TR-02-056

Stodolsky's Theorem and Neutrino Oscillation Phases—for Pedestrians
     H. J. Lipkin
          ANL-HEP-TR-02-119

Neutrino Technical Reports

Letter of Intent to Build an OffAxis Detector to Study $\nu_\mu \rightarrow \nu_e$ Oscillations With the NuMI
Neutrino Beam
     D. Ayres, G. Drake, M. Goodman, V. Guarino, T. Joff-Minor, D. Reyna,
     R. Talaga, J. Thron et al
          July 17, 2002

Accelerator Improvement Options for NuMI Proton Intensity
     B. Choudhary, T. Fields, G.W. Foster, J. Griffin, P. Lucas, A. Marchionni,
     P. Martin, D. Micheal, E. Prebys, S. Pruss
          NuMI-863, August 5, 2002

Detector R&D for Future Neutrino Experiments with NuMI Beamline
     G. Barenboim, G. Drake, M. Goodman, P. Litchfield, M. Szleper et al
          NuMI-880, October 21, 2002

CDF Notes:

CDF-6183   The CDF Run IIb Trigger Using the ATLAS Region of Interest Builder
                    R. Blair, J. Dawson, T. Liu
                    CDF/DOC/TRIGGER/GROUP/6183

CDF-6114   Efficiency of Momentum Dependent Muon Matching Cuts
                T. LeCompte
                CDF/ANAL/MUON/CDFR/6114

CDF-6106   Study of L2 EM Trigger Inefficiency at high eta
                Yanwen Liu, Ray Culbertson,Steve Kuhlmann
                CDF/DOC/EXOTIC//6106

CDF-6101   CPR Material Counts of CDF Run II
            Minsuk Kim (Kyungpook National Univ), Ray Culbertson (Fermi National Lab),
                Robert Blair (Argonne National Lab)
                CDF/PUB/CDF/PUBLIC/6101

CDF-6094   Preliminary Test on Photomultiplier Tubes for the CPR2 Detector
                S. Lami, S. Kuhlmann, K. Hatakeyama, M. Gallinaro
                CDF/PUB/CALORIMETRY/CDFR/6094

CDF-6090   On The Issue of the J/Psi Alignment
                Thomas J. LeCompte
                CDF/MEMO/BOTTOM/CDFR/6090

PDK Notes:

PDK-796   Other Atmospheric Neutrino Experiments
                M. Goodman
                Contribution to the Proceeding of the XXth International Conference on
                Neutrino Physics and Astrophysic, May 2002, Munich, Germany

PDK-797   Search for Neutron-Antineutron Oscillations Using Multiprong Events in Soudan 2
                J. Chung, W.W. M. Allison, D.S. Ayres, J. H. Cobb, T.H. Fields,
                M.C. Goodman, T. Joffe-Minor, J. L. Thron, P. Litchfield et al
                Published in Phy. Rev. **D66**, 032004 (2002).

WF-Notes:

WF-206   On the Design of Dielectric Taper Section for Epislonr=20
                Wanming Liu, July 29, 2002.

WF-207   On the Choosing of the Sample Points for Determine the External Q and Resonant
            Frequency of Wage Guide Loaded Cavities
                W. Liu, July 30, 2002.

WF-208 On the Design of Coupling Scheme for Dielectric Loaded Sstanding Wave Acceleration Cavity

     W. Liu, C. Jing, Wei Gai, August 12, 2002.

WF-209 Current Measurement on Bipolar Power Supply

     S. Yusof, October 2002.

WF-210 EM Design of Coaxial Cable to Circular Waveguide TM01 Adaptor

     W. Liu, W. Gai, November 2002.

V.   COLLOQUIA AND CONFERENCE TALKS

Edmond L. Berger

Light Bottom Squark Phenomenology and Upsilon Decay
  CLEO Collaboration Meeting, Ithaca, NY, December 13, 2002.

Higgs Production
  Illinois Institute of Technology, Chicago, November 21, 2002.

Higgs Boson Production Including All-orders Soft Gluon Resummation, Theoretical Seminar,
  CERN, Geneva, Switzerland, November 14, 2002.

Higgs Boson Production at the LHC, CMS Collaboration Seminar, CERN, Geneva, Switzerland,
  November 14, 2002.

Summary Talk - Working Group on Tests of QCD
  International Workshop on Heavy Quarkonia, Geneva, Switzerland, November 10, 2002.

Quarkonium and Supersymmetry
  International Workshop on Heavy Quarkonia, Geneva, Switzerland, November 9, 2002.

Inclusive Higgs Boson Production at LHC
  CTEQ Collaboration Meeting, Riverside, CA, October 25-26, 2002.

Light Bottom Squark Phenomenology
  International Conference on High Energy Physics, Amsterdam, July 26, 2002.

Higgs Boson Decay into Hadronic Jets
  Workshop on TeV-Scale Physics, Cambridge University, England, July 21, 2002.

Geoffrey Bodwin

Inclusive Production of Heavy Quarkonium
  Invited plenary talk, International Workshop on Heavy Quarkonia, Geneva, Switzerland,
  November 9, 2002.

Resummation of Vacuum-Polarization Corrections to Quarkonium Decay Rates
  Invited plenary talk, International Workshop on Heavy Quarkonia, Geneva, Switzerland,
  November 8, 2002.

Some Recent Results on Quarkonium Production and Decay
>Invited plenary talk, Fifth Edition of the Conference "Quark Confinement and the Hadron Spectrum" Gargnano (Brescia), Italy, September 10-14, 2002.

Inclusive Production of Heavy Quarkonium in Hadronic Collisions
>Invited plenary talk, International Conference on Advanced Topics in QCD, Beijing, PRChina, August 5-9, 2002.

John Campbell

W, Z + 2 Jet Production at Hadron Colliders
>Department of Physics, Florida State University, Tallahassee, FL, September 16, 2002.

W + 2 Jets at the Tevatron
>FNAL, Batavia, IL, July 11, 2002.

Chengwei Chiang

Phenomenology of a Light Bottom Squark in the MSSM
>Institute of Nuclear Theory, University of Washington, Seattle, WA, November 19, 2002.

Phenomenology of a Light Bottom Squark in the MSSM
>Department of Physics, University of Illinois at Chicago, October 28, 2002.

Higgs Decay Into Hadronic Jets
>Theory Institute 2002: SUSY, Higgs, and Extra Dimensions, Argonne, IL, September 11, 2002.

Wei Gai

Invited talk: "Recent Results from the Argonne Wakefield Accelerator",
>2002 Linac Conference, August 20 -2 4, Kyeongju, Korea.

Maury Goodman

The Neutrino Oscillation Industry
>Department of Physics Colloquium, Kansas University, Lawrence Kansas, September 30, 2002

Eve Kovacs

QCD Physics at CDF
> International Conference on Advanced Topics in QCD, Beijing, PRChina, August 5-9, 2002.

Harry J. Lipkin

The Application of Lie Algebras to the Separation of Degrees of Freedom in Problems with Many Degrees of Freedom
> Technische Universitaet Berlin, Germany, November 21, 2002.

Puzzles in Hyperon, Charm and Beauty Physics
> Department of Physics, University of Illinois, Urbana, October 7, 2002.

Puzzles in Hyperon, Charm and Beauty Physics
> Department of Physics, University of Rochester, NY, September 30, 2002.

Reminiscences from the Days at Cornell, MIT, Princeton, and More: When electrical engineering students were told that there was no future in electronics and physics students were told by Niels Bohr that there was no future in quantum mechanics
> Department of Physics, University of Guelph, Ontario, Canada, September 24, 2002.

Puzzles in Hyperon, Charm and Beauty Physics
> Physics Department, University of Toronto, Ontario, Canada, September 23, 2002.

Brandon Murakami

Lepton Flavor Violation through Z' Bosons
> Department of Physics, Purdue University, West Lafayette, IN, September 24, 2002.

Jim Norem

RF Induced Backgrounds in the Muon Ionization Cooling Experiment (MICE)
> NUFACT 02 Imperial College London, July 3, 2002.

Field Emission and Breakdown in Copper Cavities.
> Argonne Accelerator Science and Technology Seminar, Oct 15, 2002.

Dark Currents and Field Emission at 805 MHz
  SLAC/NLC Design Group, Oct 21, 2002.

Geraldine Servant

Kaluza-Klein Dark Matter
  Department of Physics, Yale University, New Haven, CT, December 16, 2002.

Kaluza-Klein Dark Matter
  Department of Physics, University of Minnesota, Minneapolis, October 24, 2002.

Kaluza-Klein Dark Matter
  Department of Physics, University of Illinois at Chicago, IL, October 7, 2002.

Kaluza-Klein Dark Matter
  High Energy Physics Division Seminar, Argonne, IL, September 25, 2002.

Kaluza-Klein Dark Matter
  Theory Institute 2002: SUSY, Higgs, and Extra Dimensions, Argonne, IL, September 9-13, 2002.

Kaluza-Klein Dark Matter
  Santa Fe Summer Workshop on Extra Dimensions and Beyond, NM, August 8, 2002.

Kaluza-Klein Dark Matter
  Aspen Summer Workshop, CO, July 10, 2002.

Timothy Tait

Branes and Orbifolds are Opaque
  Santa Fe Summer Workshop on Extra Dimensions and Beyond, NM, August 4-10, 2002.

Carlos Wagner

Precision Measurement and Unification of Coupling
  Caltech, Pasadena, CA, December 9, 2002.

Local Brane Kinetic Terms in Extra Dimensions
  Aspen Summer Workshop, CO, July 22, 2002.

Cosmas Zachos

Deformation Quantization of Nambu Mechanics
Invited talk presented at the 31st HEP and Cosmology Coral Gables Conference on "Short-Distance Behavior of the Fundamental Interactions", Ft. Lauderdale, FL, December 14, 2002.

Phase-Space Quantization: Quantum Mechanics Lives and Works in Phase Space
Physics Department, Purdue University, West Lafayette, November 19, 2002.

Deformation Quantization, Superintegrability, and Nambu Mechanics
Fermilab, Batavia, IL, November 7, 2002.

Phase-Space Quantization
Physics Department, University of Michigan, Ann Arbor, October 11, 2002.

Deformation Quantization, Superintegrability, and Nambu Mechanics
Invited talk presented at the Wigner Centennial Conference, Pécs, Hungary, July 12, 2002.

VI.   HIGH ENERGY PHYSICS COMMUNITY ACTIVITIES

Edmond L. Berger

Convener, Session on Polarized Gluon Density, Conference on the Physics of Spin, University of Washington, Seattle, August 4-7, 2003.

Scientific Organizing Committee, Conference on the Physics of Spin, University of Washington, Seattle, August 4-7, 2003.

Organizing Committee, 8th Conference on the Intersections of Particle and Nuclear Physics (CIPANP 2003), New York, May 19-24, 2003.

Co-organizer, Argonne Workshop on Trends in Neutrino Physics, Argonne, IL, May 12-16, 2003.

Search Committee, Argonne/University of Chicago joint faculty position 2002-2003.

Convener, International Workshop on Heavy Quarkonia, CERN, Geneva, November 8-10, 2002.

Member, International Advisory Committee, HADRON 2003, Aschaffenburg, Germany, August 31--September 6, 2003.

Member, Andrew Gemant Award Committee, American Institute of Physics, 2002--.

Member, American Linear Collider Working Group, 2002--.

Co-organizer, Greater Chicagoland Particle Theory Meeting, Argonne, IL, October 21, 2002.

International Advisory Committee, Conference in Honor of Jean Tran Thanh Van, Paris, October 2002.

Organizing Committee, Theory Institute on Supersymmetry, Higgs, and Extra-Dimensions, Argonne National Laboratory, September 9-13, 2002.

Member, CTEQ Collaboration

Adjunct Professor of Physics, Michigan State University, East Lansing, MI, 1997-present.

Scientific Program Organizing Committee, Rencontres de Moriond, QCD and High Energy Hadronic Interactions, France, every year from 1986 to the present.

Geoffrey T. Bodwin

Member, Quarkonium Working Group, 2002 --

International Advisory Committee, Fifth Edition of the Conference "Quark Confinement and the Hadron Spectrum" Gargnano, Italy, September 10-14, 2002.

Convener, Session on "Heavy Quarkonium", Fifth Edition of the Conference "Quark Confinement and the Hadron Spectrum" Gargnano, Italy, September 10-14, 2002.

Organizing Committee, International Conference on Advanced Topics in QCD, Beijing, PRChina, August 5-9, 2002.

John Campbell

Organizing Committee, Theory Institute on Supersymmetry, Higgs, and Extra-Dimensions, Argonne National Laboratory, September 9-13, 2002.

Cheng-Wei Chiang

Organizing Committee, Theory Institute on Supersymmetry, Higgs, and Extra-Dimensions, Argonne National Laboratory, September 9-13, 2002.

Wei Gai

Committee: Scientific Advisory and Organizing Committee, Advanced Accelerator Concepts Workshops, Oxnard, CA 2002, and Stony Brook, NY, 2004.

Maury Goodman

Member Particle Data Group

International Advisory Committee, Neutrino 2004 conference (Paris)

Nominations Committee, Forum on Physics and Society of the American Physical Society

Investments Committee of the American Physical Society

Editor, Long-Baseline Newsletter

Jing Jiang

Organizing Committee, Theory Institute on Supersymmetry, Higgs, and Extra-Dimensions, Argonne National Laboratory, September 9-13, 2002.

Jungil Lee

Organizing Committee, Theory Institute on Supersymmetry, Higgs, and Extra-Dimensions, Argonne National Laboratory, September 9-13, 2002.

Harry Lipkin

Member, International Advisory Committee, HADRON 2003, Aschaffenburg, Germany, August 31--September 6, 2003.

Award Recipient, The Wigner Medal, Paris, July 18, 2002.

Brandon Murakami

Organizing Committee, Theory Institute on Supersymmetry, Higgs, and Extra-Dimensions, Argonne National Laboratory, September 9-13, 2002.

Geraldine Servant

Organizing Committee, Theory Institute on Supersymmetry, Higgs, and Extra-Dimensions, Argonne National Laboratory, September 9-13, 2002.

Tim Tait

Organizing Committee, Theory Institute on Supersymmetry, Higgs, and Extra-Dimensions, Argonne National Laboratory, September 9-13, 2002.

Carlos Wagner

Head, Theory Committee, Argonne National Laboratory, 2003--

Organizer, Baryogenesis Workshop, U Michigan, Ann Arbor, June 9-27, 2003.

Co-organizer, Argonne Workshop on Trends in Neutrino Physics, Argonne, IL, May 12-16, 2003.

Search Committee, Argonne/U Chicago Joint Faculty Position, 2002--2003.

Co-organizer, Greater Chicagoland Particle Theory Meeting, Argonne, IL, October 21, 2002.

Organizing Committee, Theory Institute on Supersymmetry, Higgs, and Extra-Dimensions, Argonne National Laboratory, September 9-13, 2002.

Head, Theory Group, HEP Division, Argonne National Laboratory, September 2002—

Local Organizer, Cosmo02 Conference, Chicago, IL, September 2002.

Associate Professor, Lecturer for Courses on Supersymmetry and Advanced Electrodynamics, U Chicago, IL, 2000--2003.

Member, LEP Higgs Working Group, 1997--2002.

Cosmas Zachos

Member, Advisory Panel, J. Phys A: Math Gen (IOP).

VII.   HEP DIVISION RESEARCH PERSONNEL

Administration

Price, L.   Hill, D.

Accelerator Physicists

Conde, M.   Norem, J.
Gai, W.   Power, J.
Schioessow, P.   Yusof, Z.

Experimental Physicists

Ayres, D.   Nodulman, L.
Blair, R.   Proudfoot, J.
Byrum, K.   Repond, J.
Cadman, R.   Reyna, D.
Chekanov, S.   Spinka, H.
Derrick, M.   Stanek, R.
Fields, T.   Talaga, R.
Goodman, M.   Tanaka, M.
Joffe-Minor, T.   Thron, J.
Krakauer, D.   Underwood, D.
Kuhlmann, S.   Wagner, R.
LeCompte, T.   Wicklund, A.
Magill, S.   Xia, L.
May, E.   Yokosawa, A.
Musgrave, B.   Yoshida, R.

Theoretical Physicists

Berger, E.   Servant, G.
Bodwin, G.   Sinclair, D.
Campbell, J.   Tait, T.
Chiang, C. W.   Wagner, C.
Jiang, J.   White, A.
Lee, J.   Zachos, C.
Murakami, B.

Engineers and Computer Scientists

Dawson, J.	Hill, N.
Drake, G.	Kovacs, E.
Grudzinski, J.	Mouser, C.
Guarino, V.	Schlereth, J.
Gieraltowski, J.	Vaniachine, A.

Technical Support Staff

Adams, C.	Konecny, R.
Ambats, I.	Matijas, Z.
Anderson, S.	Nephew, T.
Cox, G.	Reed, L.
Cundiff, T.	Haberichter, W.
Farrow, M.	Rezmer, R.
Franchini, F.	Skrzecz, F.
Kasprzyk, T.	Wood, K.

Laboratory Graduate Participants

Loizides, J.	Jing, C.
Miglioranzi, S.	

Visiting Scientists

Kovacs, E. (Theory)	Lipkin, H. (Theory)
Krueger, K. (STAR)	Ramsey, G. (Theory)
Liu, W. (AWA)	Uretsky, J. (Theory)